Hindawi
Journal of Nanomaterials
Volume 2019, Article ID 5942194, 31 pages
https://doi.org/10.1155/2019/5942194

Review Article

Metaloxide Nanomaterials and Nanocomposites of Ecological Purpose

Tetiana A. Dontsova, Svitlana V. Nahirniak, and Ihor M. Astrelin

Department of Inorganic Substances, Water Purification, and General Chemical Technology, National Technical University of Ukraine "Igor Sikorsky Kyiv Polytechnic Institute", Kyiv 03056, Ukraine

Correspondence should be addressed to Tetiana A. Dontsova; dontsova@xtf.kpi.ua

Received 28 November 2018; Revised 3 March 2019; Accepted 14 March 2019; Published 30 April 2019

Guest Editor: Ziyou Zhou

Copyright © 2019 Tetiana A. Dontsova et al. This is an open access article distributed under the Creative Commons Attribution License, which permits unrestricted use, distribution, and reproduction in any medium, provided the original work is properly cited.

The features of the properties and creation of nanocomposite metal oxide materials, especially TiO_2, ZnO, SnO_2, ZrO_2, and Fe_3O_4, and their applications for ecology are considered in the article. It is shown that nanomaterials based on them are very promising for use in the ecological direction, especially as sorbents, photocatalysts, and sensitive layers of gas sensors. The crystallochemical characteristics, surface structure, and surface phenomena that occur when they enter the water and air environment are given for these metal oxides, and it is shown that they play a significant role in obtaining the sorption and catalytic characteristics of these nanomaterials. Particular attention is paid to the dispersion and morphology of metal oxide particles by which their physical and chemical properties can be controlled. Synthesis methods of metal oxide nanomaterials and ways for creating of nanocomposites based on them are characterized, and it is noted that there are many methods for obtaining individual nanoparticles of metal oxides with certain properties. The main task is the correct selection and testing of parameters. The prospects for the production of metal oxide nanocomposites and their application for environmental applications are noted, which will lead to a fundamentally new class of materials and new environmental technologies with their participation.

1. Introduction

Nanomaterials based on metal oxides (nanostructured and nanodispersed) are a diverse class of materials in terms of electronic structure and physical, chemical, and electromagnetic properties [1]. The application of metal oxide nanomaterials and nanocomposites based on them is becoming increasingly popular in applied ecology, especially where they can be used as adsorbents and photocatalysts as well as a material for the manufacture of environmental monitoring devices. Adsorption materials based on nanosized metal oxides have a large specific surface area, high capacity, fast kinetics, and specific affinity for various contaminants [2–5]. The use of nanostructured metal oxides in photocatalytic processes allows the oxidation of organic compounds that are not decomposed biochemically, and the pretreatment of aqueous solutions by their use is considered to be the most promising [2, 6, 7]. Metal oxide nanostructures used in environmental monitoring as sensitive layers of chemoresistive gas sensors are characterized by high values of the sensory signal due to the large specific surface area; hence, a higher adsorption capacity [8–10].

Consequently, nanosized metal oxide materials are of considerable interest because of significant advantages over bulk analogues and, of course, because they have great prospects for obtaining new types of adsorbents, photocatalysts, and sensitive layers of gas sensors based on them. However, nanostructured and nanodispersed oxides also have a significant drawback—their application can lead to environmental pollution with nanoparticles. In this case, it is promising to create metal-oxide nanocomposites—an extremely interesting type of nanomaterial due to their properties—that may exceed the properties of its individual phases by order. The use of the latter will prevent the loss of metal oxide nanoparticles due to the stabilization of the nanoparticles in the composite's matrix, which will also positively affect the separation process after the completion of the processes of sorption and photocatalysis [4]. In addition, nanocomposites due to their

structure have special, sometimes unique, physical and chemical properties, and they can be applied in a wide variety of fields, including the production of new materials for use in the fields of medicine, energy, and ecology.

The purpose of this work is to consider the features and potential use of the metal oxide nanomaterials and nanocomposites based on TiO_2, ZnO, SnO_2, ZrO_2, and Fe_3O_4 for environmental applications. The crystallochemical structures of selected metal oxides, the features of their surface structure, and their possible surface phenomena in water and air environments are considered in the article. Their physical, chemical, sorptive, and photocatalytic properties are also provided for an understanding of their more efficient usage. We also reviewed what we considered the most promising synthesis methods of individual oxides in terms of ease of implementation, and the existing approaches for the creation of nanocomposite metal oxide materials of ecological direction in the literature are presented.

2. Crystallochemical Characteristics of Metal Oxides and Their Surface Structure

2.1. Crystallochemical Structures of TiO_2, ZnO, SnO_2, ZrO_2, and Fe_3O_4. In nature, TiO_2 exists in three different crystalline structures: rutile, anatase, and brookite. In all modifications, the structural unit of the TiO_2 crystalline lattice is the distorted TiO_6 octahedra, joined together by common vertices or ribs, i.e., each Ti^{4+} ion is surrounded by six O^{2-} ions, and each O^{2-} ion is surrounded by three Ti^{4+} ions. Octahedra are arranged in such a way that each oxygen ion belongs to three octahedra [11]. In rutile, the octahedra of TiO_6 are connected with two adjacent octahedra along the edges in the (001) plane, resulting in longitudinal bands in the crystal lattice. In anatase, the octahedra of TiO_6 are connected along the edges lying in the (001) and (100) planes. Thus, each octahedron has four common ribs with neighbors that form zigzag chains. There are 4 common ribs for one octahedron in anatase and 2 in rutile. Hence, the elementary cell of anatase consists of four TiO_2 molecules, while that of rutile consists of only two (see Figure 1).

At atmospheric pressure and temperature, anatase is less dense and less stable than rutile. In the brookite structure, each octahedron of TiO_6 has two common ribs with its neighbors and also forms zigzag chains. The Ti–O bond lengths in these structures are 0.195-0.198, 0.194-0.197, and 0.187-0.204 nm for rutile, anatase, and brookite, respectively [12]. The parameters and some characteristics of all of the TiO_2 modifications are shown in Table 1.

When heated, both anatase and brookite irreversibly transform into rutile. The temperature transition depends on many factors, including impurities, the obtainment method, the precursor type, and the size of the final crystal. Also, the direct obtainment of the particular phase can be realized by adjusting the finite particle size [13].

Zinc oxide crystallizes in three modifications: hexagonal wurtzite, cubic sphalerite, and cubic modification of the NaCl type, which is rare. Only the hexagonal wurtsite is thermodynamically stable under normal conditions. Cubic sphalerite can be obtained when growing ZnO on the substrates with a cubic lattice. ZnO with the NaCl structure is obtained at relatively high pressures [14].

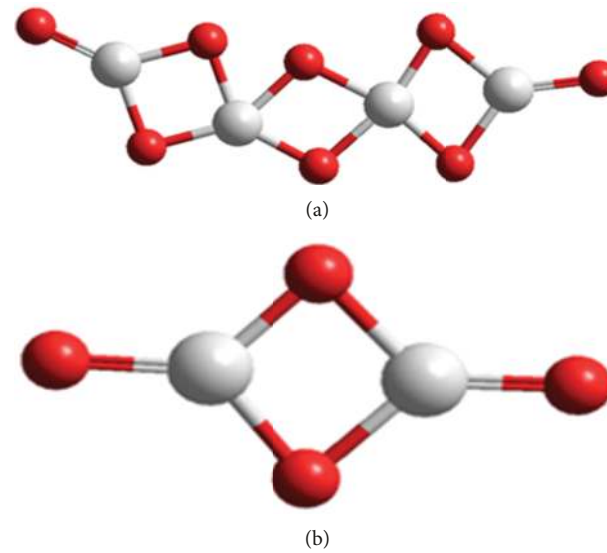

Figure 1: Elementary cells of rutile (a) and anatase (b): titanium—white; oxygen—red.

The wurtsite structure is obtained from the hexagonal close-packed lattice consisting of two interpenetrating packed hexagonal Bravais lattices based on the positions (0 0 0) and $(a/2\sqrt{3a/c}\ c/2)$. In the ideal tetrahedral surroundings, the constants a and c are correlated with each other as $c/a = \sqrt{8/13}$. In real structures, there are deviations from this relationship. The ZnO structure can be described as the series of alternating planes composed of tetrahedrally coordinated O^{2-} and Zn^{2+} arranged one on top of another along the c axis. O^{2-} and Zn^{2+} form the tetrahedral unit, and the whole structure is devoid of central symmetry (see Figure 2). [15].

SnO_2 has only one stable phase, the mineral form of which is known as cassiterite. Tin (IV) oxide crystallizes in the tetragonal structure of rutile, the parameters and characteristics of which are given in Table 1. In the rutile structure, tin atoms are located at the center and surrounded by six oxygen atoms, which are located at the corners of the almost regular octahedron. Atoms of oxygen are surrounded by three tin atoms, which form an equilateral triangle. The length of the Sn–O bond is 0.209-0.216 nm [16, 17].

ZrO_2 also exists in three crystalline modifications (see Figure 3): monoclinic, tetragonal, and cubic. The cubic ZrO_2 has a fluorite structure, in the crystal lattice of which each zirconium atom has eight bonds with oxygen atoms. Thus, zirconium atoms form face-centered cubic lattices with oxygen atoms occupying the position in tetrahedral interstices. Consequently, the elementary cell of cubic ZrO_2 contains one zirconium atom and two atoms of oxygen; the length of the Zr–O bond is 0.221 nm [18, 19].

The tetragonal ZrO_2 can be considered as a slightly distorted cubic structure (see Figure 3(b)). In the crystalline tetragonal structure of ZrO_2, zirconium atoms are also bound to eight oxygen atoms—four neighboring oxygen atoms are located at the tetrahedron plane with a Zr–O bond length of 0.207 nm, while the other oxygen atoms are located at a

Table 1: Parameters of TiO_2, ZnO, SnO_2, ZrO_2, and Fe_3O_4 crystalline lattices and some of their characteristics [11, 14–16, 19, 23].

Phase	Space group	Lattice parameters (nm)	Volumetric density (g/cm^3)	Band gap (eV)
TiO_2 tetragonal (rutile)	P4/mnm	$a = 0.4585$, $c = 0.2953$	4.3	3.0
TiO_2 tetragonal (anatase)	I4/amd	$a = 0.3784$, $c = 0.9515$	3.9	3.2
TiO_2 rhombic (brookite)	Pbca	$a = 0.9184$, $b = 0.5447$, $c = 0.5145$	4.1	3.3
ZnO hexagonal	$P6_3mc$	$a = 0.3249$, $c = 0.5206$	5.6	3.4
SnO_2 tetragonal (cassiterite)	$P4_2/nmm$	$a = 0.4738$, $c = 0.3188$	7.0	3.6
ZrO_2 monoclinic (baddeleyite)	$P2_1/c$	$a = 0.5169$, $b = 0.5232$, $c = 0.5341$	5.6	5.8
ZrO_2 tetragonal	$P4_2/nmc$	$a = 0.514$, $b = 0.527$, $a/c = 1.02$ (at 1523 K)	6.1	5.8
ZrO_2 cubic	Fm/3m	$a = 0.5256$ (at 2603 K)	6.3	6.1
Fe_3O_4 cubic (magnetite)	Fd/3m	$a = 0.8396$	5.2	~2

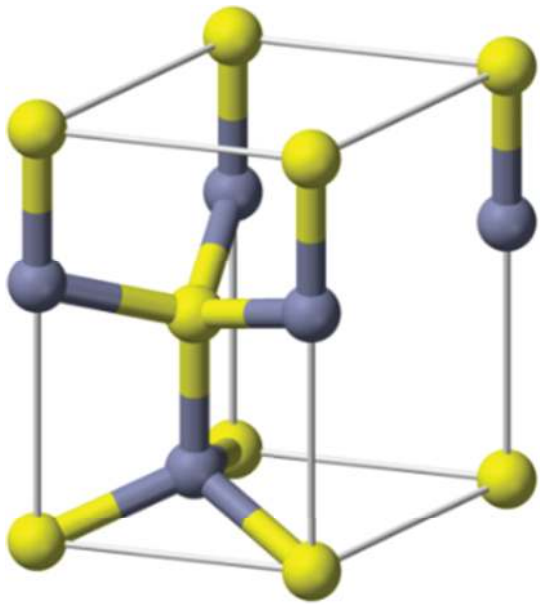

Figure 2: Elementary cell of wurtzite: zinc—violet; oxygen—yellow.

90° angle to the tetrahedron plane at a distance of 0.246 nm from the zirconium atoms [19, 20]. The monoclinic ZrO_2 is formed by further distortion of the tetragonal structure (see Figure 3(c)). It is even less symmetric and is represented by 12 atoms of an elementary cell and more complex geometric structures. In the monoclinic ZrO_2, zirconium atoms have seven bonds with oxygen. In the space, the oxygen atoms form angles of 134.5° and 109.5°. Consequently, the atoms of oxygen are not in the same plane. In the crystalline structure of the monoclinic ZrO_2, the interatomic distances of Zr–O vary considerably; however, they have average values of 0.207 nm and 0.221 nm [20, 21]. Some structural characteristics of ZrO_2 are given in Table 1.

The monoclinic ZrO_2 modification is the most stable, and transition to it occurs during cooling from 1273 K to 923 K. On the contrary, during heating, the monoclinic phase is transformed into a tetragonal modification, starting at 1093 K. At the same time, the tetragonal modification exists even up to 1443 K [22]. Consequently, the tetragonal ZrO_2 modification is unstable and can be stabilized by using dopants (usually rare earth oxides, calcium, magnesium, and iron). Cubic ZrO_2 has the highest strength and density. However, the like tetragonal modification, it is also unstable. To stabilize the cubic modification, the same dopants for the tetragonal modification are used; however, larger amounts are used.

Magnetite belongs to the class of spinel, which has the general formula AB_2O_4, where A and B are cations of divalent and trivalent metals, respectively. The structure of spinel is based on the face-centered cubic lattice with oxygen atoms, in which 1/8 tetrahedral and 1/2 octahedral positions are occupied. Magnetite has the structure of an inverse spinel, in which the elementary cell contains 32 oxygen anions with 64 tetrahedral and 32 octahedral cavities, where the Fe (III) ions are randomly distributed between the octahedral and tetrahedral positions, and the Fe (II) ions are found only in the octahedral positions [23, 24]. The parameters of the magnetite crystalline lattice and some of its characteristics are presented in Table 1.

2.2. Features of the Metal Oxide Surface Structure. The surface of metal oxides plays a major role in adsorption processes, heterogeneous (photo)catalysis, detection of molecules in the gas environment, etc., since in these cases all molecular and chemical processes occur on the surface of metal oxide crystals. The surface is considered as the transition region from the crystal volume to the environment that is in contact with the atmosphere, which leads to the formation of oxide layers, depositions on the surface, or penetration into the water vapor, carbon atoms, and other chemical compounds. Therefore, the actual surfaces of the crystals are too complicated to study, so it is usually assumed that they are atomically clean and smooth surfaces, which are considered as simplified models of real systems.

To a certain extent, they are similar to bulk crystals in terms of their structural properties and reactivity surfaces; however, there are a number of differences that can fundamentally distinguish their surface from that of bulk crystals. These consist of the arrangement of atoms and ions, which is different from the location found in bulk crystals; the ionic mobility of the particles on the surface; the number and nature of defects and dislocations; the presence of surface groups with different chemical compositions on them; the

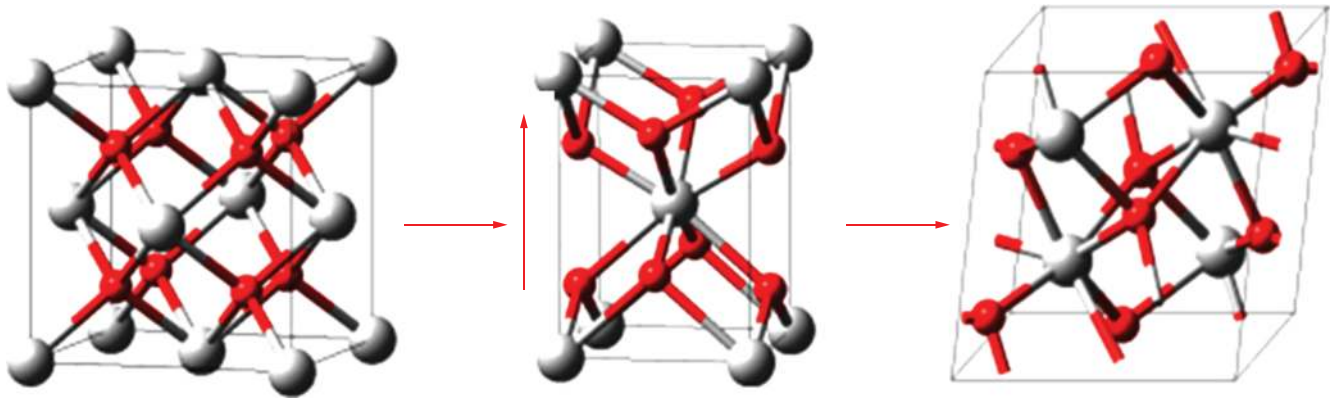

Figure 3: Distortion of ZrO_2 crystalline lattices: cubic (a), tetragonal (b), and monoclinic (c).

ability of the surface for adsorptive concentration of matter from adjacent volumetric phases; and the wider set of possible structures corresponding to this solid material than in the volume [25]. Also, chemical bond types that are unique or rarely encountered can be realized on the surface. This is due to the following factors: the presence of the phase separation boundary, which sharply differs in electrical and chemical properties; the reduction of symmetry on the surface, which facilitates the appearance of attenuated, intermediate, and deformed bonds; the presence of defects in the structure, as well as mechanical stresses, resulting in the redistribution of electronic density; and finally, the incomplete saturation of bonds in the surface structures [25]. So, proceeding from this, the surface is the special state of matter with its chemistry.

Many papers were preoccupied in both experimental and theoretical studies of the surface structure and its influence on the TiO_2 properties [11, 26–48]. The results of these studies indicate that the definition of the surface structure of TiO_2 and defects on it is rather the complex issue, especially because of the presence of Magneli phases, which for TiO_2 fluctuates between Ti_2O_3 and TiO_2 [44, 45]. In addition, titanium (IV) oxide is characterized by a variety of TiO_2 crystalline structures; hence, in the first place, the structure of its surface will be determined by the phase composition.

The main building unit of titanium (IV) oxide structures is Ti_2O_4 or Ti_4O_8. In all three structures of titanium (IV) oxide, the scaling is carried out by the multiplication of octahedra for the triple-coordinated oxygen atom $O^{(3)}$. The features of the structure of bulk crystals of rutile and anatase and the most thermodynamically stable faces (110) and (101) are shown in Figures 4(a) and 4(b).

From Figure 4, it is evident that both surfaces have six and five times coordinated atoms of titanium $Ti^{(6)}$ and $Ti^{(5)}$, and triple- and double-coordinated atoms of oxygen $O^{(3)}$ and $O^{(2)}$ [42, 46–48]. The presence or absence of the latter (the so-called bridge oxygen atoms) can change the electronic structure of the bulk material and the surface energy of the faces; hence, the finite properties of TiO_2.

The ZnO surface is studied by examining faces $(10\bar{1}0)$ and $(11\bar{2}0)$ [49]. At the same time, the physical and chemical properties of ZnO are primarily affected by their own defects caused by the absence or presence of zinc or oxygen in the lattice [50]. Therefore, in the case of ZnO, the surface structure and its properties primarily depend on its stoichiometry.

The surface of zinc oxide is the most studied $(10\bar{1}0)$ (see Figure 5). In the stoichiometric ZnO, the shortening of the Zn–O bond from 0.198 nm to 0.183 nm is observed due to the surface relaxation on this face. As a result, a slight transformation occurs, in which the surface zinc "gets involved" inside the structure, and oxygen "appears" above the surface. In the case of the nonstoichiometric zinc oxide, everything is more complicated; as a result, the surface may have fundamentally different properties.

In the SnO_2 single crystals, low-index facets (110) and (101) are the most developed. The surface (110) is the most theoretically [51–57] and experimentally [58–70]studied. The surface structure and the presence of these or other facets to a decisive extent depend on the methods and conditions of SnO_2 synthesis, which in turn affects the concentration of oxygen on the surface in the lattice. The production of SnO_2 crystals in the absence of oxygen leads to the formation of the oxygen-depleted (110) face.

The face (101) in the SnO_2 single crystal has been studied only recently [71–75]. In this case, the double valence of tin contributes to the formation of different charges on this face: Sn^{2+} or Sn^{4+}. The transition from one charge to another on this face is easily accomplished through the peculiarity of atomic stacking in this crystallographic direction. The structure of the (101) surface is shown on Figure 6. It can be seen that atomic stacking along this direction can be described as the three-layer O–Sn–O, the boundary of which is oxygen (see Figure 6(a)); that is, with such a sequence, tin retains its valence for Sn^{4+}. When removing the oxygen layer, the surface of the crystal is already ending with the layer of tin (see Figure 6(b)); as a result, the transformation of Sn(IV) into Sn(II) can easily take place [76]. Thus, the addition or removal of the surface oxygen layer by simply treating it at ambient conditions or in vacuum, can convert the tin surface from Sn(IV) to Sn(II) or vice versa. For the face (110), such easy conversion is not observed; therefore, on this face tin exists only in the form of Sn(IV) [71, 76].

In the environment, the pure ZrO_2 phase has the monoclonal structure of the baddeleyite m-ZrO_2 [77, 78], in

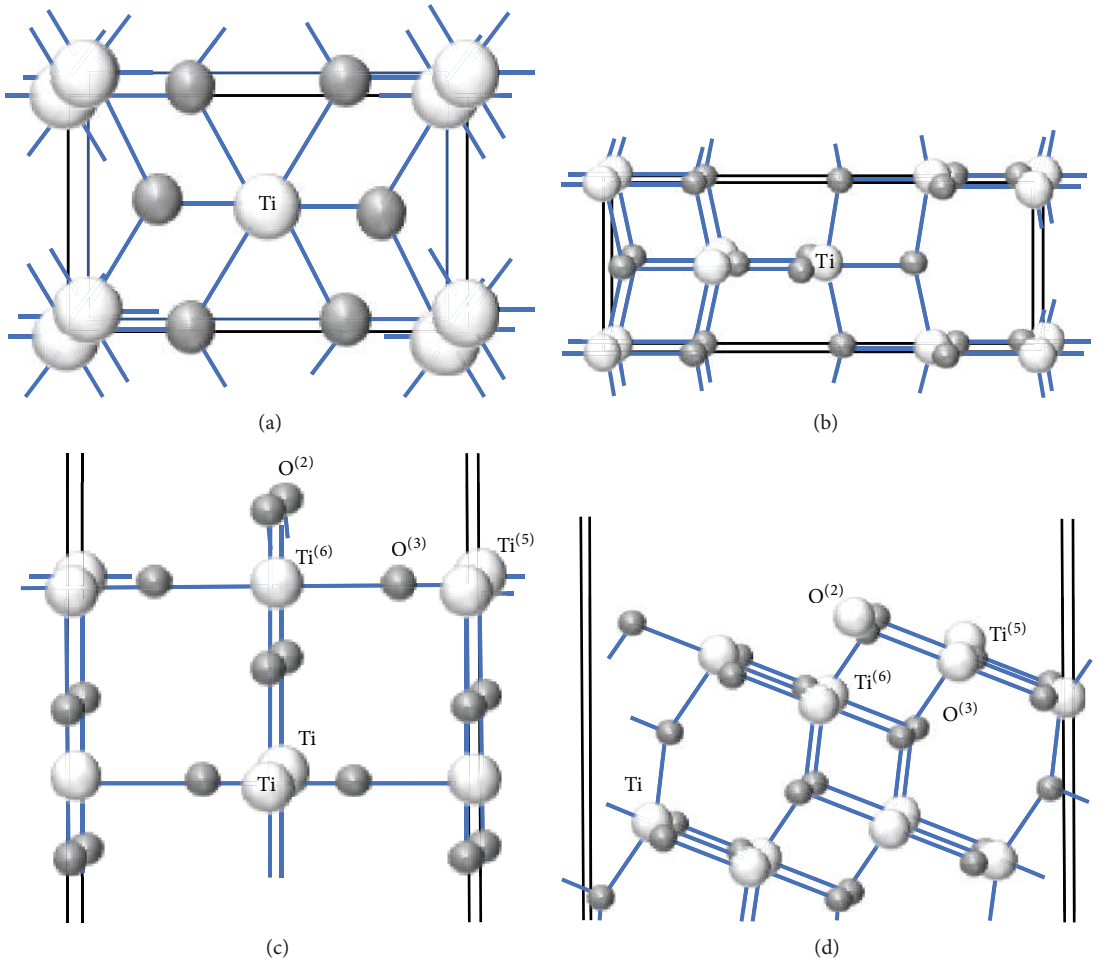

FIGURE 4: The structure of the bulk structures of rutile (a) and anatase (b) and faces (110) and (101) of rutile (c) and anatase (d), respectively.

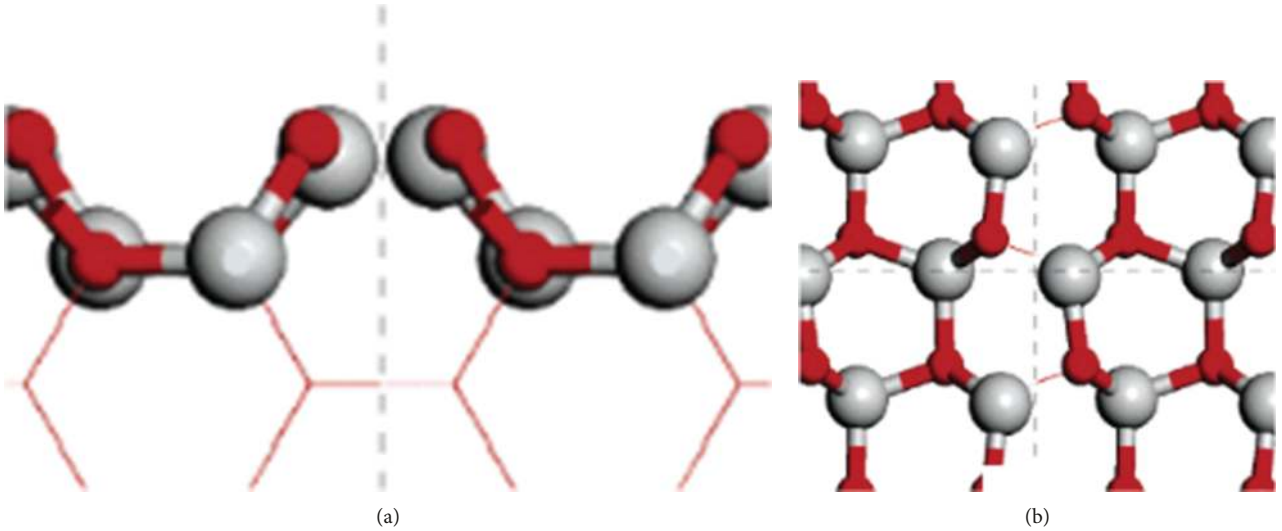

FIGURE 5: The structure of the stoichiometric $(10\bar{1}0)$ surface: (a) side view and (b) top view [49].

which zirconium is in a distorted sevenfold coordination, and oxygen atoms are four times or three times coordinated (see Figures 7(a)–7)c)). At approximately 1400 K, m-ZrO_2 is transformed into the tetragonal structure (t-ZrO_2), where zirconia is surrounded by eight anions but with two different Zr–O distances. The ideal eightfold coordination with the transformation of t-ZrO_2 into the cubic structure of the fluorite type (c-ZrO_2) is achieved at 2600 K [79–81].

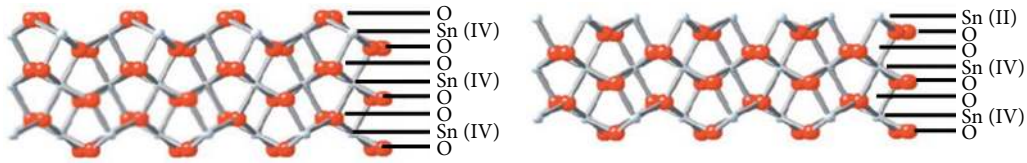

(a) (b)

FIGURE 6: Structure of the (101) facet of three layers on the SnO_2 surface (cross-section) (a) with the existing boundary oxygen layer (110) and (b) without it.

Experimental studies of ZrO_2 polycrystalline samples have shown that only a few crystal faces with low indices are open, especially the face (101), which is the most stable (see Figures 7(d) and 7(e)), and (001) [77, 82–85]. Theoretical studies have confirmed the discovered fact. Figures 7(d) and 7(e) show three outer layers where dashed lines allocate the repeating link of one layer in the direction perpendicular to the surface. The oxygen atoms have threefold coordination on these surfaces, and there are two different types of oxygen atoms on the face (101).

The structure of magnetite is based on the tight packet of oxygen (anion of the lattice) with iron cations, occupying octahedral and tetrahedral coordinated gaps between them (see Figure 8), in which Fe (II) and Fe (III) coexist in the octahedral position. Properties of magnetite are mainly determined by this fact.

Natural and synthetic crystals of Fe_3O_4 often have octahedral crystals, in which the main facet is (111) [23]. However, depending on the synthesis conditions, it is possible to obtain other forms of magnetite particles, for example, cubes (see Figure 9), in which the main facet is (100). Consequently, the properties of magnetite can be regulated by obtaining magnetite particles of different shapes, which will have the different set of surface facets; therefore, they will differ in surface energies.

In the (100) direction, the surface of magnetite consists of layers, which alternate as follows: the first layer consists of two Fe (III) ions in the tetrahedral position, then the plane containing eight O^{2-} anions followed by two Fe (III) ions and two Fe (II) ions in the octahedral positions (see Figure 10(a)). The main defect of this face may be an excess of iron ions [23].

The direction (111) in the magnetite consists of 6 different atomic planes: iron in the tetrahedral positions of Fe_{tet1}, plane of oxygen O_1, iron in the octahedral positions of Fe_{oct1}, plane of oxygen O_2, iron in the tetrahedral positions of Fe_{tet2}, and iron in the octahedral positions of Fe_{oct2} (see Figure 10(b)). Consequently, the close location of the oxygen plane to the surface causes a strong negative charge, but the presence of iron in the tetrahedral positions of Fe_{tet1} partially neutralizes it, resulting in the formation of the polar surface on the facet (111) by Tasker type 3 surfaces [23, 24, 86, 87].

The considered structures and structural features of different surfaces of TiO_2, ZnO, SnO_2, ZrO_2, and Fe_3O_4 indicate that the control of the metal oxide properties, especially in the nanodispersed range where the surface comes to the fore, begins with the shape and size of the crystals that affect the presence of those or other facets depending on the choice of the synthesis method, the process conditions, and treatment parameters after obtaining them.

2.3. Surface Phenomena on Metal Oxides. The phenomena occurring on the surface of solids are traditionally described using several models: statistical, band, and geometric [25, 88].

The statistical model (the model of "local" interactions) is based on the chemical approach, in which surface phenomena are described through active centers belonging to the surface. The active centers in this case are the surface atoms of the lattice, centers connected with defects of an inhomogeneous surface (point defects, dislocations), and impurities on the surface. When considering the surface in the theory of the crystalline field, the surface centers are free orbitals with a high affinity to the electron or occupied orbitals with a low ionization potential. Thus, the active centers are always localized on the real surface of the solid and have certain chemical activities [25].

A band model ("hard zone" model) is based on the electronic or energy approach. In this model, the surface description is carried out through surface states, which correspond to the surface electronic energy levels. The corresponding mathematical description does not depend on the chemical nature of the adsorbate and on the details of the local chemical interaction. The description is carried out due to the energy position in the forbidden zone of the semiconductor, which changes its charge depending on the position of the Fermi level on the surface.

The geometric model is based on the geometric characteristics of the surface, and the latter is considered as the fractal structure characterized by fractional dimensionality (D) and repeatability on different scales. For example, if $D = 2$, then this is a perfectly smooth surface, and if $D = 3$, then we are talking about volumetric porous structures. The fractality of the surface has a significant effect on its properties, for example, on sorption and catalytic characteristics, etc. [88]. At a later time, all these models are taken into account more increasingly when considering the surface phenomena involving metal oxides [89–95].

The acid-base properties of metal-oxide systems, which exhibit practically all the fundamental parameters of a solid, reflect the surface reactivity in the best way. According to this, two types of acidic and basic centers, the Lewis center and the Brønsted center, can exist on the surface of the solid. The presence of acidic and alkaline centers (as well as water) on the surface will determine the chemical activity of the solid as an adsorbent, (photo)catalyst, or metal oxide semiconductor [96].

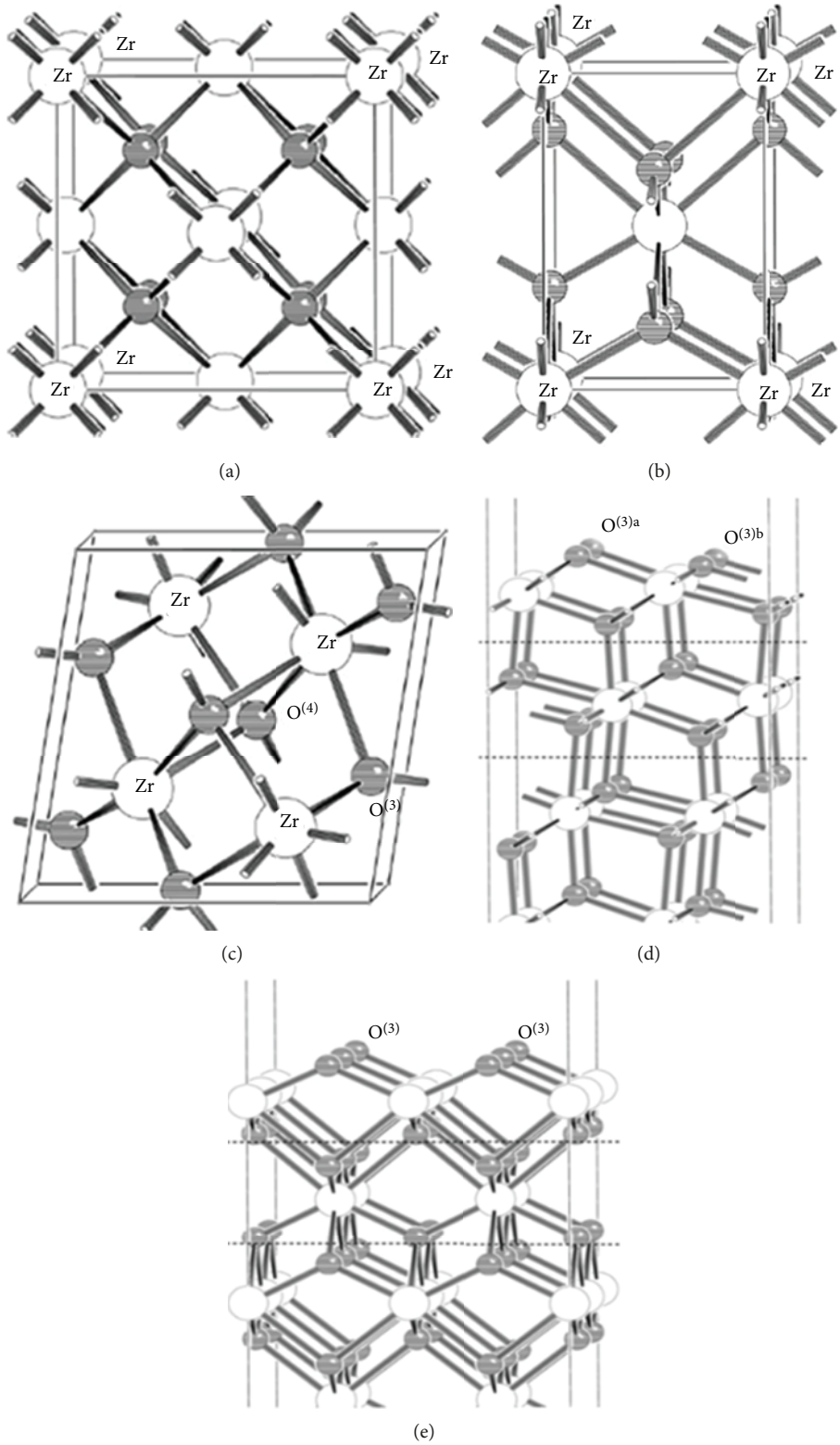

FIGURE 7: Bulk ZrO_2 crystals of various polymorphic modifications: cubic (a), tetragonal (b), and monoclinic (c). The most stable faces (101) (d) and (001) (e) on the t-ZrO_2 surface. White balls—oxygen; gray—zirconium [77].

The Lewis acid center is the vacant metal atom or the localized surface state capable of accepting an electron pair or an electron donating a molecular fragment. The alkaline Lewis centers are formed from the orbital of an oxygen atom on the surface and interact with the electron transfer to the energy level of the adsorbed molecule. Thus, any cation

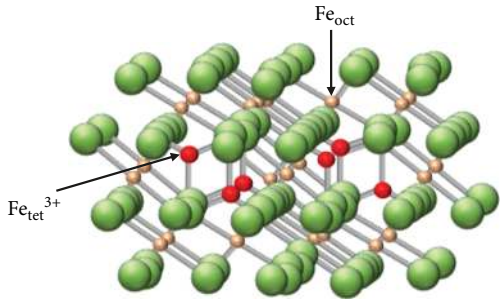

Figure 8: The structure of magnetite (green balls—oxygen, yellow balls—iron in octahedral gaps, and red balls—iron in tetrahedral gaps).

having unfilled electronic orbitals is an acid by the Lewis definition, and each of the surface anions having an undivided electron pair is an alkaline center [97].

Along with the aprotic centers (or the Lewis centers), there are proton acids and the Brønsted bases on the surface of the solid, which are the result of the interaction of water molecules and their fragments with aprotic centers. In the case of the adsorption of water molecules on one-electron surface levels formed by the homolytic dissociation mechanism, the Brønsted acids and bases of different acidic strengths can be formed, depending on which type of surface state participated in this process—the Shockley state (see Figure 11(a)) or the Tamm state (see Figure 11(b)). In the case of the interaction of water molecules with acids and bases of the Lewis centers, two types of mechanisms are possible: dissociative (see Figure 11(c)) and molecular (see Figure 11(d)). The molecular mechanism is also realized in the hydration process of the solid due to the water adsorption at the Brønsted acid and base centers by alkaline (see Figure 11(e)) and acid (see Figure 11(f)) types [97].

In the literature, the interaction of the surfaces of amphoteric metal oxides, which also include TiO_2, ZnO, SnO_2, ZrO_2, and Fe_3O_4, with water in aqueous medium, is described by a simplified mechanism [98–101]:

$$\begin{aligned} &\mathrm{MeOH} + \mathrm{H^+} \leftrightarrow \mathrm{MeOH_2^+}, \quad \text{if pH of solution} < \mathrm{pH_{pzc}},\\ &\mathrm{MeOH} + \mathrm{OH^-} \leftrightarrow \mathrm{MeO^-} + \mathrm{H_2O}, \quad \text{if pH of solution} > \mathrm{pH_{pzc}}, \end{aligned} \tag{1}$$

where pH_{pzc} is the point of zero charge.

Figure 12 shows the scheme of the interaction of the metal oxide surface with oxygen in the air.

In this case, according to studies of electron paramagnetic resonance, the adsorbed oxygen may be present on the surface of metal oxides in various chemical forms, the formation of which occurs according to the following scheme [102]:

$$\mathrm{O_{2(g)}} \rightarrow \mathrm{O_{2(ad)}} \rightarrow \mathrm{O_2^-{}_{(ad)}} \rightarrow \mathrm{O^-{}_{(ad)}} \rightarrow \mathrm{O^{2-}{}_{(ad)}} \rightarrow \mathrm{O^{2-}{}_{(lat.)}}. \tag{2}$$

The temperature dependence of the existence of this or that oxygen form was established in [103], where it is indicated that the transition from adsorbed oxygen to chemosorbed oxygen ($\mathrm{O_{2(ad)}} \rightarrow \mathrm{O_2^-{}_{(ad)}}$) occurs approximately at 423 K. The significant reduction in the conductivity of metal oxide systems at temperatures higher than 423 K was connected with this.

2.4. Properties of Metal Oxides in the Different States of Dispersion and Morphology. Metal oxides form the basis of modern diverse intellectual materials and devices due to the possibility of controlling their physical and chemical properties. Their properties depend on many chemical and structural characteristics: chemical composition, various defects, morphology, particle size, specific surface area, etc. By changing any of these characteristics, the electrical, optical, magnetic, (photo)catalytic, and sorption properties can be controlled. The unique characteristics of metal oxides make them the most diverse class of materials covering almost all aspects of material science and physics in the fields of semiconductivity, superconductivity, ferroelectricity, and magnetism [102].

The nanostructured titanium (IV) oxide has high chemical and thermal stability, and with special doping by impurity levels in an electronic structure, it is uniquely capable of the creating new functional materials on itself, especially for (photo)catalysis, sensors, adsorption, and photovoltaics. The highly dispersed doped TiO_2 for the creation of a photocatalyst that would work efficiently in the visible spectrum, as well as the components of devices for the efficient conversion of solar energy into electricity (solar cells), is of particular interest [104–109].

In the process of using nanodispersed, submicron and micron ZnO for bleaching methylene orange in aqueous solutions, the following order was revealed: nanodispersed powder (50 nm) > submicron powder (200 nm) > micron powder (1000 nm) [110]. The authors explain the fact as follows: the number of dispersed nanoparticles per volume in the reaction solution increases, and consequently, the photon absorption ability is improved; the large surface area of the nanodispersed powder contributes to the large adsorption of dye molecules on the catalyst surface; and the recombination process is reduced due to the smaller path of electrons and holes on the surface of the particles.

Tin (IV) oxide is one of the classical sensory materials that belong to the class of substances that combines high electrical conductivity and optical transparency in the visible spectral region, has chemical stability at high temperatures, etc. [111]. Therefore, materials based on SnO_2 are widely used as organic oxidation catalysts, lithium ion batteries, transparent electrodes of solar cells, various electronic and optical coatings, and as sensitive materials for metal oxide chemoresistive gas sensors.

Modifications of nanodispersed ZrO_2-based nanomaterials determine the ways of application, since each of its modifications has a number of properties inherent only for that particular modification. The monoclinic modification of ZrO_2 nanopowders is used mostly in the production of substrates for luminescent, photosensitive materials [112]; in catalysis [113, 114]; and in the production of nanomaterials

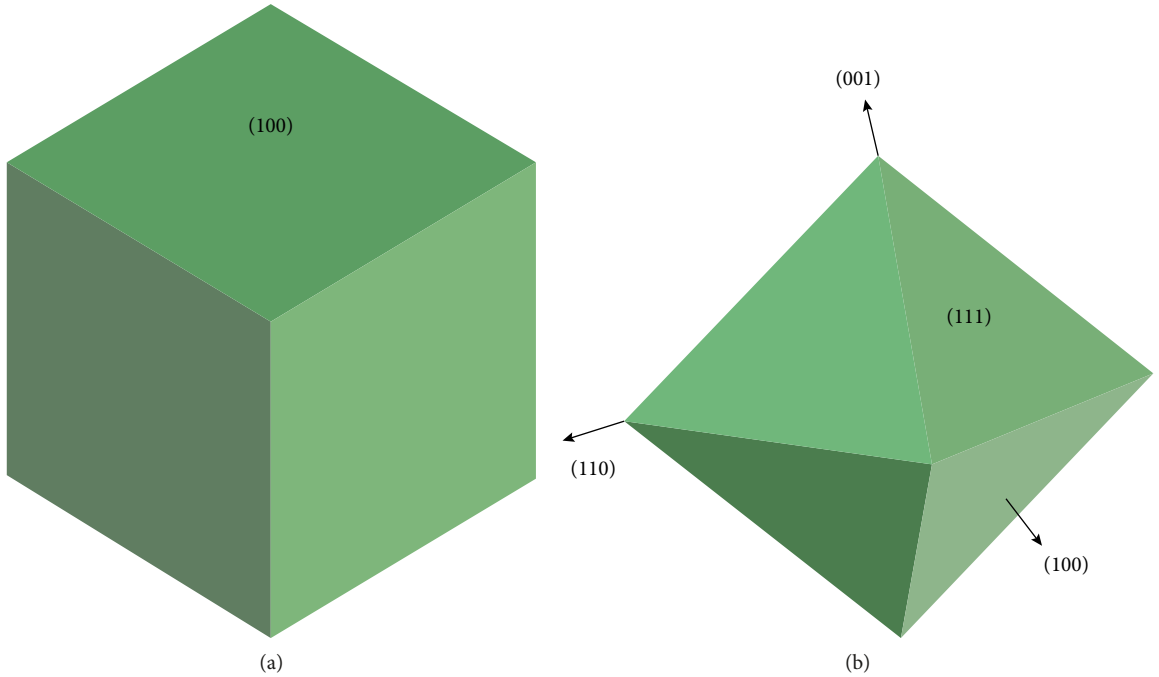

Figure 9: Magnetite particles in the form of the cube (a) and octahedron (b) [23].

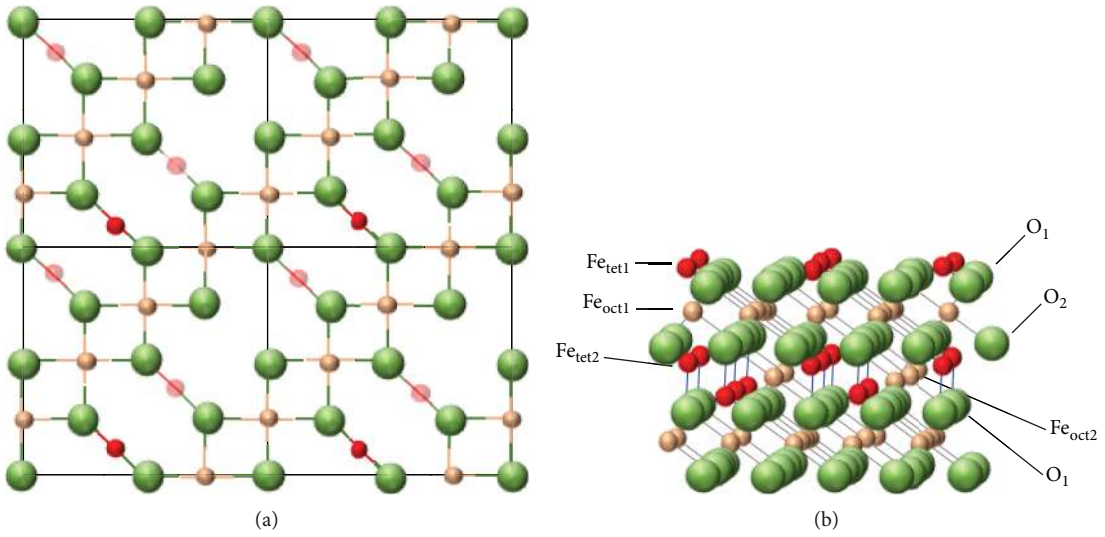

Figure 10: The structure of Fe_3O_4 surfaces: (a) the top view of the facet (100), where Fe_{tet} is red, Fe_{oct} is yellow, and oxygen is green; (b) side view of the facet [23].

based on tetragonal and cubic ZrO_2 modifications, for example, in ceramic materials, including new materials with improved performance [115]. The tetragonal modification of zirconium (IV) oxide has become widely used for bioceramics in restorative dentistry [116, 117] and in catalysis [118, 119], and its cubic modification has become widely used for chemically resistant and thermostable high-strength nanoceramics [120] and for solid electrolytes in solid oxide fuel cells [121, 122].

The constantly growing interest in the properties of nanomagnetism is due to its powerful potential for solving a wide range of tasks in material science, mineralogy, biology, and medicine [123]. At present, the application of magnetic nanoparticles is the most widely developed in biology and medicine, storage and recording of information, and in other areas of science and technology. At sizes from several to tens of nanometers, magnetic particles, especially nanomagnetic particles, reveal the special characteristic of their magnetic behavior—superparamagnetism. Recent studies have shown that the prospective application of magnetite is in sorption technology, since it has been found that it has a high sorption activity for some organic compounds, and the modification of existing sorption materials allows removing them quickly by magnetic separation [124, 125].

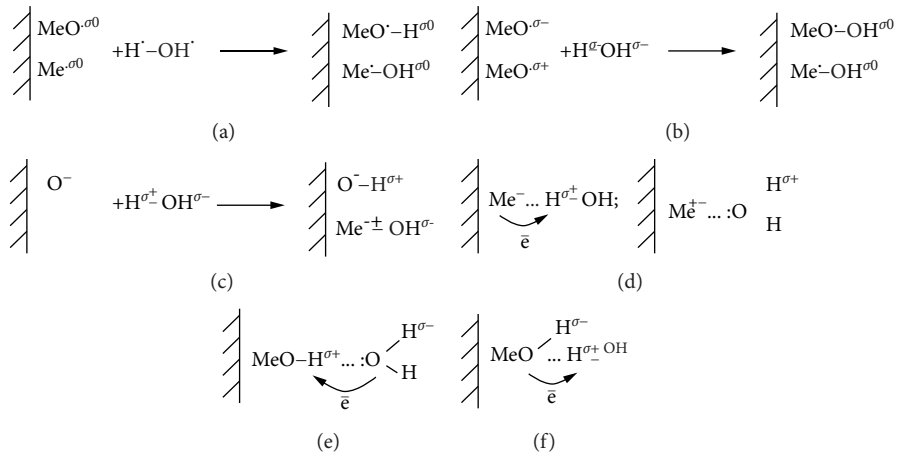

Figure 11: Mechanisms of the interaction of water with different centers on the surface of metal oxides.

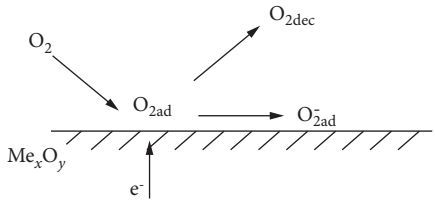

Figure 12: Schematic formation of the chemosorbed oxygen on the surface of metal oxides.

Consequently, the considered multifaceted properties of these nanostructured and nanodispersed metal oxides make these materials very promising not only for optical and electronic applications, but also for their use in environmental applications, which is the cause for the significant scientific interest in them by environmental engineering specialists.

2.5. Features of Chemical and Physical Characteristics in the Nanodispersed Range. Materials obtained from nanosized particles exhibit unusual chemical and physical properties that differ significantly from the properties of the respective bulk materials. Their study is important in modern science, because such studies are fundamental, since they allow investigating the changes in the properties of substances in the gradual transition from atomic or molecular level to condensed systems.

The peculiarities of the chemical and physical characteristics of nanoparticles related to their size are determined by the following phenomena. With a decrease of the particle size, the percentage of atoms on the surface increases. This leads to the increase in reactivity due to coordination nonsaturation. Proceeding from this and taking into account the fact that with the transition to nanoparticles the surface-to-volume ratio increases, the origin of these "unusual" properties, called "dimensional effects," becomes clear.

The influence of the particle size on the physical and chemical properties of the substance is also due to the presence of surface pressure acting on the substance. This additional pressure, which is inversely proportional to the particle size, leads to the increase in the Gibbs energy and, consequently, increases the pressure of the saturated vapor above the nanoparticles and decreases the boiling point of the liquid and the melting point of the solid phase. Other thermodynamic characteristics also change, especially the equilibrium constant and the standard electrode potentials [126]. Also, when the size of the particles decreases, the influence of the structure on the stoichiometry of the material is noticeably manifested [127]. A variation of stoichiometry leads to a significant change in the chemical and (photo)catalytic activities of the material.

For example, when the size of the titanium (IV) oxide particle diminishes, its anatase modification becomes more stable and, according to the results of studies [128–130], the anatase structure has a greater number of oxygen vacancies on the surface than the rutile structure. This results in its greater chemical and photocatalytic activities compared to rutile.

When reducing the size of ZnO particles to nanometer size, some of its physical properties undergo changes that are known today as "quantum size effects." For example, quantum confinement increases the energy gap of quasi-one-dimensional (Q1D) ZnO, which is confirmed by photoluminescence. The band gap of ZnO nanoparticles also demonstrates the same dependence [131]. In this case, ZnO can be used to create unique nanostructures that are in demand in a wide variety of applications, such as in optoelectronics, sensors, transducers, and photocatalytic and biomedical materials. From this, it follows that ZnO unambiguously has the richest family of nanostructures among all materials, which differ in both structure and properties [132].

As already mentioned, materials based on zirconium (IV) oxide have different applications depending on the phase composition. In particular, monoclinic ZrO_2 is used as a catalyst [113, 114], tetragonal ZrO_2 is used as a carrier of catalysts [118, 119], and cubic ZrO_2 is used as a solid electrolyte in fuel cells of solid oxide batteries [121, 122]. The degree of tetragonality or cubicity at normal temperatures depends on the size of the crystallites: the metastable tetragonal modification of ZrO_2 can be obtained under normal conditions if the size of the crystallites is less than 25-30 nm, and the metastable cubic ZrO_2 modification can be obtained if the crystallite size is less than 5-10 nm [133].

The change in the physical and chemical properties of SnO_2 and Fe_3O_4 in the transition to the nanoscale is achieved by varying the morphology of these nanoparticles, which determines the presence of certain facets on the surface, which differ in their surface energies [23, 76].

2.6. Sorption, (Photo)catalytic, and Sensory Properties of Metal Oxides. One of the most important properties of metal oxide nanoparticles, which has a large potential for application in various chemical and technological processes, is their high adsorption capacity in relation to pollutants in water systems, especially organic matter, which indicates the prospect of using metal oxide nanomaterials to improve the ecological state of the environment. A similar impressive adsorption capacity of metal oxide nanoparticles and other compounds to various organic compounds has been documented by many researchers [133–138]. A significant increase in catalytic activity was found in some metal oxides in the transition to the nanoparticles [138–140].

The dimensional effect is already widely used in heterogeneous catalysis. In many cases, the nanoparticles exhibit catalytic activity where the same larger particles are inactive. The explanation for these phenomena is based on the acid-alkaline properties of metal oxides, which change in the transition to the nanoscale, namely, a large number of active centers are exposed, which is connected, first of all, to the sharp increase in the specific surface area. When obtaining these metal oxides in the form of nanostructures, the percentage of coordinated-unsaturated ions, especially at the edges and angles of microcrystallites, is predicted to be large. Consequently, the physical and chemical properties of the surface in such nanoscale systems will play a decisive role in determining the scale of their application and in assessing the catalytic activity.

Controlled regulation of the functional properties of metal-oxide nanomaterials and the implementation of the dependencies of composition-structure-properties can also be accomplished by changing the phase composition, which in many respects also determines their physical and chemical characteristics.

2.6.1. TiO_2. The most important of all applications of different crystalline modifications of TiO_2 is the ecological direction, namely, in the sorption-photocatalytic processes. Along with crystalline modifications, the amorphous TiO_2 modification is also actively synthesized and studied. However, the latter has no photoactivity but has high sorption properties. At the same time, the sorption-photocatalytic properties are influenced by such parameters as the degree of crystallinity, the correlation between modifications, the distribution of particles in size and shape, the specific surface area, and the average pore size.

Among the three polymorphic modifications of titanium (IV) oxide, only rutile and anatase have an applied value. Rutile is a more thermodynamically stable structure; however, anatase is considered to be more promising as a nanomaterial of the ecological direction due to the greater photochemical activity. However, there are data in the literature on the increase of the photocatalytic activity of TiO_2-based nanomaterials when they consist of mixed phases, such as anatase and brookite or anatase and rutile [141]. Due to the denser packing of ions in crystals, rutile exceeds anatase in terms of stability, density, hardness, refractive index, and dielectric permittivity, but it is believed that it has insufficient photochemical activity [142–144]. In recent scientific publications [145, 146], there is evidence that brookite, an unstable modification of TiO_2, is characterized with the highest photocatalytic activity. Unfortunately, it is difficult to obtain this modification in pure form even in laboratory conditions.

Despite that the band gap in rutile (3.0 eV) is lower than that in anatase (3.2 eV), the latter crystalline modification still has the higher photocatalytic activity. This is explained by the fact that anatase is a semiconductor with an indirect forbidden zone, and rutile, in turn, is a semiconductor with a direct width of the forbidden zone. As a result, in anatase, electrons and holes can migrate from volume to the surface at a high rate, which leads to a low recombination rate [147]. Typically, the mixture of these modifications gives higher photocatalytic activities compared to individual modifications due to the synergistic effects that are manifested in the interfacial interaction and electron transfer [148–150]. For example, when using the mixture of anatase and rutile, the recombination of photogenerated electrons and holes decreases due to the anatase modification, and light absorption increases due to rutile.

2.6.2. ZnO. Due to the unique electrical, optical, and mechanical properties and the remarkable characteristics in electronics, optics, and photonics, ZnO can be effectively used in environmental applications, namely, as a photocatalyst and a sensor material.

As a photocatalyst, zinc oxide is already competing with the most popular catalyst based on TiO_2, which holds leading positions not without a base. Recently, however, in-depth research in the scientific literature on the ZnO-based photocatalyst for the destruction of various pollutants in aqueous solutions shows the significant promise of this oxide for use along this direction [111]. It is noted that the creation of a "suitable" ZnO architecture during synthesis will allow minimizing the loss of the electron during excitation and maximizing the absorption of photons [151–153]. Among other things, its nontoxicity and ecological purity are noted, which are very important for such materials that are used for environmental purposes [111]. Thus, by varying the morphology and particle size, it is possible to create effective photocatalysts for wastewater treatment.

Zinc oxide has proved itself as a promising sensitive material for gas sensors because of its high surface conductivity in various environments. At the same time, this parameter strongly depends on the morphology and size of ZnO particles. It is established that the use of ZnO nanowhiskers, nanowires, nanorods, and nanobelts as well as the nanoflower architecture significantly increases the surface conductivity [154, 155].

2.6.3. SnO_2. The sensitivity of sensors based on metal oxides strongly depends on the morphology of their particles [156].

In this sense, one-dimensional nanostructures such as nanowires and nanobelts are of greatest interest [157–161]. Sensors based on them are promising because of the possibility of creating sensors of ultrahigh sensitivity ppb-level sensors. The authors [162] theoretically proved and experimentally confirmed that the sensitivity of one-dimensional nanostructures is much larger than that of nanoparticles with a round shape and depends on two important parameters: (1) the particle surface-to-volume ratio and (2) the Debye radius. It has been shown that the characteristics of metal-oxide sensors strongly depend on the size and morphology of nanostructures.

2.6.4. ZrO_2. Zirconium (IV) oxide is used as the catalyst (due to the greater number of acidic centers on the surface) in the monoclinic modification [163], as the carrier for catalysts (due to the high thermal stability) in the tetragonal modification [164], and as the sorbent in the amorphous phase or at a low degree of crystallinity [165, 166].

When zirconium (IV) oxide is used as a catalyst, the acid-alkaline nature of its properties and the presence of several types of defect in the crystalline lattice and on the surface, which is one of the main factors of the reactive-catalytic activity of the surface of any oxide, play an important role. When using ZrO_2 as the carrier for catalysts, it must have sufficiently developed outer and inner surfaces. These requirements are provided to obtain zirconium (IV) oxide crystallites with a size as little as possible. One of the most unusual and promising properties of zirconium (IV) oxide particles is their sorption capacity both to anions and cations, which allows considering nanosized ZrO_2 and materials based on them as instruments for improving the ecological state of the environment. In this case, the hydrated zirconium (IV) oxide that is in the amorphous state has the highest sorption capacity [165, 166]. The specificity of ZrO_2 usage as the sorbent is that it has high selectivity to polyvalent anions (chromates, borates, sulfates, phosphates, arsenates, etc.) and can be used at high temperatures without losing its effectiveness.

The ZrO_2 cubic modification is used as an oxygen sensor. The high thermal stability of the zirconium (IV) oxide cubic modification and the ability of the sensors based on it to operate in hot, contaminated, and wet gases without any additional preparation makes ZrO_2 a promising material for the creation of sensors operating in difficult conditions. In this case, the use of ZrO_2 and materials based on it in the nanoband allows increasing the surface area of the sensor material (solid electrolyte), resulting in the receipt of high-sensitivity sensors to oxygen [167].

2.6.5. Fe_2O_3. Magnetite is considered as a promising nanomaterial for use in water purification due to its high surface-to-volume ratio, magnetic properties, and the possibility of easy surface modification and reuse [168]. Because of the listed advantages, it has enormous potential for application in the ecological direction as a sorbent, photocatalyst, and modifier. Particularly noteworthy is its magnetic properties, which contribute to the creation of more effective water purification schemes by combining adsorption with magnetic separation, which is becoming widespread in the field of water treatment [169, 170]. In addition, magnetite has a relatively lower cost, high sorption capacity, and stability [171–173]. Current applications of nanomagnetite, which are predicted in water purification, can be divided into two groups: technologies that use magnetite as the nanosorbent or the modifier for faster removal of the used sorbent (adsorption technologies) and technologies that use magnetite as the photocatalyst to destroy contaminants or convert them into less toxic forms (photocatalytic technologies) [171]. However, it can be assumed that technology based on the usage of nanomagnetite will soon be used employing both approaches at the same time.

2.7. Optical, Electrical, and Magnetic Properties. As has been shown in numerous studies [174–179], the optical, electrical, and magnetic properties of metal oxides depend on their dispersion and morphology. Thus, there is an increase in electrical resistance and permittivity observed in nanophase metal oxide systems compared to metal oxide macrosystems [180], and TiO_2 nanoparticles absorb ultraviolet light much more efficiently than micrometer-sized particles [181]. The invented phenomena are undoubtedly related to the dimensional effects.

The dimensional effects depend on the nanoparticle size: it can either be classical (the changes in properties can be explained only by the influence of the surface) or quantum (changes in the properties of the substance cannot be interpreted as ordinary surface phenomena, most often such effects are observed for very small particles, the size of which does not exceed 10 nm) dimensional effects. It is the latter that directly affects the change in the optical, electrical, and magnetic properties of substances in the transition to the nanoscale.

Quantum dimensional effects are manifested in materials that have dimensions that are comparable to one of the characteristic lengths—the free path of charge carriers, the De Broglie wavelength, the size of the magnetic domains and the exciton, etc. [182, 183].

The change in optical properties occurs in nanoparticles with a size that is much smaller than the De Broglie wavelength and does not exceed 10-15 nm. The differences in absorption spectra in these nanoparticles and in massive objects are due to the difference in their dielectric constant [184].

The increase in the electrical resistance is due to the increasing role of defects in nanoparticles and the features of the phonon spectrum. A noticeable change in the electrical resistance is observed at particle sizes of less than 100 nm [185]. In semiconductors, the approaching of particle size to 10 nm or less leads to the decrease in the band gap (Eg) to the dielectric level [186].

The magnetic properties of particles in the nanorange change significantly. In this case the ferro- and superparamagnetic properties are manifested. Superparamagnets are magnetic only when the field is applied, while ferromagnets have a constant mean magnetic moment and stronger magnetic properties [187].

The morphology also has a significant effect on the physical and chemical properties of nanoparticles. It is generally accepted that 1D nanostructures are ideal objects for

studying the phenomenon of nanosized materials and investigating the dependence of structural properties on their size and dimension for practical use [188]. It is also expected that 1D nanomaterials, with their large specific surface area and quantum retention effects, exhibiting unique properties in contrast to their bulk analogues, will play an important role in the development of optical, electrical, electrochemical, and electromechanical devices of nanoscale dimensions [189, 190]. Management of the determined size, crystallinity, and composition of 1D nanostructures can lead to the acquisition of new properties that are impossible in the case of macromaterials [190, 191].

2.8. Optical Properties. Zinc oxide and tin (IV) oxide have unique optical characteristics. ZnO and SnO_2 belong to the group of materials that are called transparent conductive oxides. These oxides are characterized by a wide band gap $Eg > 3$ eV and are highly transparent in the visible spectrum. In this regard, they are used in the manufacture of a wide range of photovoltaic devices, such as semiconductor LEDs and solar and electrochromic cells [192]. The optical properties of pure zinc oxide and tin (IV) oxide are influenced by the degree of crystallinity of the material, the presence of point defects, and tensions in the crystal structure. These parameters affect the absorption and transmittance in the visible region of the spectrum, which are important for using them as transparent conductive oxides, especially for creating transparent electrodes. The optical properties of materials based on ZnO and SnO_2 are regulated by their doping.

2.9. Electrical Properties. Among the metal oxides under consideration, TiO_2, ZnO, and SnO_2 are characterized by electronic conductivity, which has the applied value. These electrical properties are of great importance when using these oxides as photocatalysts, sensitive layers of gas sensors, solar cells, and electrochromic devices. The conductivity of these materials is carried out both on its own (internal defects) and by impurity (doped atoms) carriers. The global growth in the demand for energy-efficient and compact devices stimulates the deep interest of researchers in this class of materials. The uniqueness of materials based on TiO_2, ZnO, and SnO_2 is that they are n-type wide-gap semiconductors that can be doped to high concentrations, turning them into degenerate semiconductors, that is, metal like. The transport in these polycrystalline materials is more complicated than in corresponding single-crystal materials. However, they are preferentially used because of their special characteristics, for example, the fact that TiO_2 is characterized by a high refractive index in the visible part of the spectrum and a high chemical and thermal stability and the fact that tin (IV) oxide has the highest chemical stability, which is a prerequisite for several applications, for example, in electrochemical elements [193].

Thus, titanium (IV) oxide has the greatest practical importance in photocatalytic processes, zinc oxide is widely used both as a photocatalyst and as sensitive layers of gas sensors, and tin (IV) oxide holds the greatest potential as a sensitive layer for miniature gas sensors. It should be added that all of them are used in the listed areas, and the creation of nanocomposites based on them is considered as the most promising direction in obtaining photocatalysts and sensory layers [194].

The authors in [195] have shown that when using TiO_2 particles in the form of nanotubes for photoelectric applications, the vector charge transfer (Figure 13) is facilitated in comparison with round-shaped nanoparticles, which leads to faster kinetics and more efficient photoelectrocatalytic degradation for three different models of disperse azo dyes in aqueous solutions [196, 197].

In addition, TiO_2 nanotubes are characterized by high sorption-photocatalytic properties (see Figure 14) [198]. According to the data given in [198], the sorption properties of TiO_2 nanotubes considerably exceed the sorption properties of the commercial nanodispersed TiO_2 sample.

Due to the fact that the hexagonal structure of ZnO does not have symmetry with respect to inversion, this leads to additional piezoelectric properties in the oxide. Like most II-VI materials, ZnO predominantly has ionic bonds, which explains its strong piezoelectric properties [14].

SnO_2 is the material that combines high electrical conductivity with such functional properties as high optical transparency in the visible spectral region and chemical stability at high temperatures [199, 200]. A high sensitivity is predicted when using 1D type SnO_2 nanostructures in sensory elements due to the higher values of the specific surface area compared to the round-shaped particles. As a result of the high values of the specific surface area, a large part of the adsorbed molecules from a gas medium will be concentrated on the surface. Thus, a reaction between the target gas and the chemically active chemisorbed molecules (O^-, O^{2-}, H^+, and OH^-) on the surface of 1D structures may occur at low temperatures [201].

Among the three zirconium (IV) oxide modifications, only the cubic modification has ionic conductivity, which determines its use in such a promising direction as the production of solid oxide fuel cells [202, 203]. The versatility of the materials based on the cubic zirconia (IV) oxide is that when introducing additional atoms (Mg, La, and Y) during the ZrO_2 synthesis the latter obtained a large number of point defects in the crystalline lattice which are associated with oxygen vacancies. This fact contributes to the growth of the ionic conductivity of cubic ZrO_2 and leads to the leveling of its dielectric properties. It should be added that doping not only changes the crystalline structure of ZrO_2 but also changes its electronic structure, which also increases ionic conductivity and, besides its application in fuel cells, finds a demand for the creation of oxygen sensors [204, 205].

2.10. Magnetic Properties. The magnetic properties of nanosized magnetite depend on many factors, including the type and defects of the crystal lattice, the size and shape of the particles, the presence of impurities, and the nature of the interaction of the nanoparticle with the surrounding matrix or other nanoparticles [206]. It has been proven that reducing the size of magnetite particles leads to qualitative changes in its magnetic properties to a one-domain state and superparamagnetism [207]. The behavior

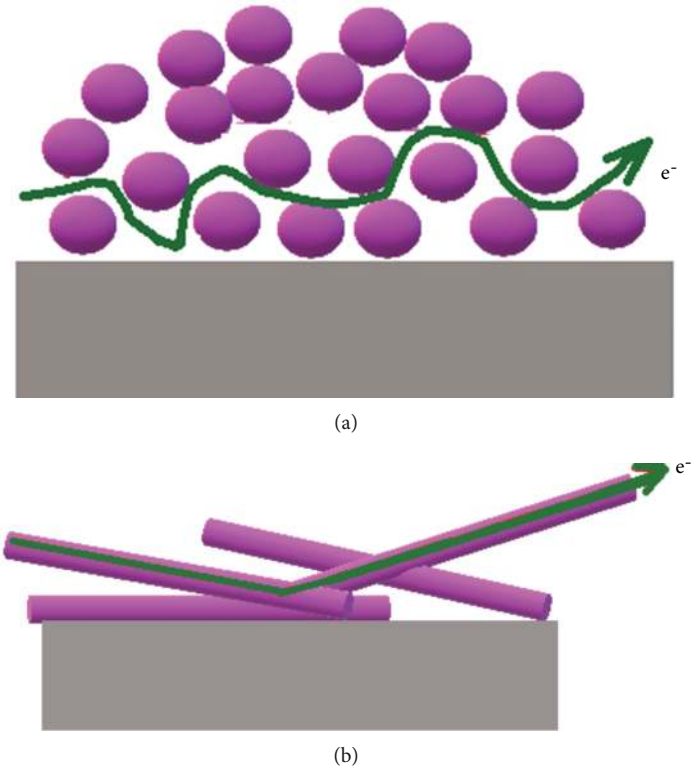

Figure 13: Nanostructured (a) and nanotube (b) photocatalytic films and the vector transport of electrons in them.

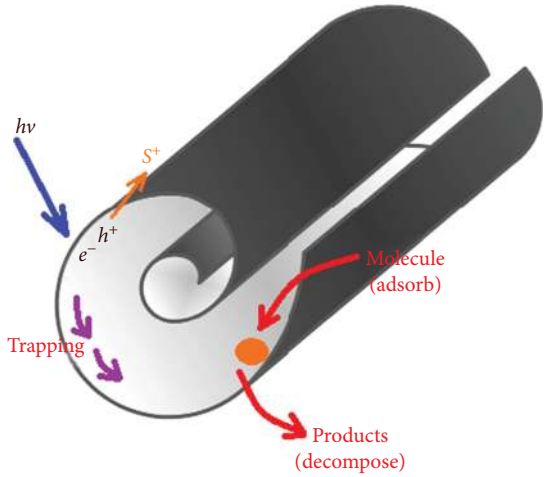

Figure 14: The TiO_2 nanotube structure and the scheme of the adsorption-photocatalytic process based on it.

of superparamagnetic substances (the size of magnetite up to 5 nm) in the external magnetic field is significantly different from ordinary paramagnets and ferromagnets. Under the influence of the external field, each separate magnetic domain takes the same direction as the external field [208]. In such systems, the losses at absorption and release of the energy of the external magnetic field are minimized, which makes them the ideal basis for magnetic resonance contrast mean in MRI studies and the magnetic modifiers of sorption materials.

Consequently, based on the considered physical, chemical, optical, electrical, sorption, photocatalytic, and magnetic properties of metal-oxide nanomaterials at various states of dispersion and morphology, the prospects and relevance of the further development of the newest effective nanomaterials based on TiO_2, ZnO, SnO_2, ZrO_2, and Fe_3O_4 for environmental applications in order to develop new environmental technologies of their use can be argued.

3. Synthesis Methods of Metal Oxide Nanomaterials and Nanocomposites Based on Them

3.1. Synthesis of Metal Oxide Nanomaterials. A synthesis method is crucial for the development of new nanomaterials, especially for the purpose of their specific applications. It affects not only the shape and size of the obtained particles but also the nanostructure, morphology, degree of crystallinity, etc., which leads to the different finite physical and chemical properties (sorption, (photo)catalytic, magnetic, and optical) of nanomaterials.

Chemical deposition, hydrothermal synthesis, sol-gel technology, gas-phase synthesis (vapor transport or CVD), template method, electrochemical synthesis, electrospinning, "green" technology, combined techniques, and others [138, 209–212] are used for obtaining metal oxide nanomaterials.

The widespread use of chemical deposition, hydrothermal synthesis, sol-gel technology, or the so-called soft chemistry methods [213] in scientific research is associated with

the relative ease of their implementation and the wide range of control parameters, such as process duration, concentration of reactants, and low temperature and pressure. In addition, to produce metal oxide products with more diverse properties, these methods can be easily combined with each other or various additional treatments can be used. For example, ultrasound or ultra-high-frequency radiation is used with the main methods of synthesis to exert influence on such properties of metal oxide nanoparticles such as size, morphology, specific surface area, and sorption capacity. Ultrasonic processing makes it possible to avoid the consolidation of formed particles and to achieve a high level of homogeneity [214, 215].

Synthesis of metal oxides from the gas phase provides a means for obtaining monocrystalline metal oxide nanoparticles of controlled and diverse morphologies with a high degree of crystallinity [216–220] with relatively high productivity, simplicity, and accessibility.

Synthesis methods of metal oxide nanoparticles, such as the electrochemical method, electrospinning method, environmental methods, or the so-called "green" technologies, are used for purely specific applications or are still in the initial stage of laboratory studies [209–212].

3.1.1. Chemical Deposition Method. The chemical deposition method is the simplest method for obtaining various substances and is based on the interaction of water-soluble or other solvents of metal compounds (usually chlorides, oxychlorides, or nitrates) with precipitators (alkali metal hydroxides, ammonia, or their oxalates). As a result, the insoluble compounds (precursors for the synthesis of nanodispersed metal oxide particles) are formed, which are subsequently washed, separated, and calcined under certain conditions to obtain the product with given properties. Even though chemical deposition is considered to be the simplest, in reality, it is a complex physicochemical process that has several stages, each of which has a significant effect on the properties of the final product [221]. By this method, it is possible to vary the properties and morphology of the resulting particles in a wide range, but the disadvantage of this method is the complexity of controlling the particle size distribution.

3.1.2. Homogeneous Deposition Method. To overcome this shortcoming, the so-called homogeneous deposition method has recently been proposed, where the precipitant and the deposited substance are in the same phase (solution) and do not interact chemically. The interaction process occurs only due to the additional chemical reaction, for example, the reaction of the carbamide hydrolysis as the mixture is heated. As a result, ammonium hydroxide is formed, which enters the deposition reaction. In this case, unlike heterogeneous deposition, the entire amount of the precipitant appears simultaneously, which prevents local supersaturation in the reaction mixture. The degree of supersaturation depends on the concentration of reagents and the heating temperature, which affects the size of the obtained particles [222]. The sediments obtained by this method are characterized by less polydispersity and greater homogeneity than in the case of the heterogeneous deposition.

3.1.3. Hydrothermal (Solvothermal) Method. The essence of the hydrothermal (solvothermal) method is to heat the aqueous (or nonaqueous) solutions of the initial reagents at a temperature above the solvent boiling point (but usually up to 573 K) in special reactors—autoclaves lined with Teflon. Processing time varies from 10 minutes to 48 hours. During the heating process, there is an increase in the pressure of saturated vapor above the solution to values greater than 0.1 MPa. Since the process is carried out in a closed system, the hydrothermal (solvothermal) method using aqueous (or nonaqueous) solutions as the reaction medium is environmentally friendly. As precursors in hydrothermal synthesis, both inorganic and organic metal salts can be used [223, 224]. At high pressure, the dissolved metal salt in water or in another solvent is converted into metal oxide, bypassing the step of converting salt into hydroxide:

$$2\mathrm{Me(NO_3)_2} + 2\mathrm{H_2O} = 2\mathrm{MeO} + 4\mathrm{HNO_3}. \quad (3)$$

A necessary condition for the course of this reaction is to carry out the process at a temperature higher than that of the area of the hydroxide existing on the P-T diagram. In addition, the properties of the reagents (solubility, diffusion rate, and reactivity) also change at elevated temperatures.

The hydrothermal (solvothermal) method allows obtaining metal oxide nanoparticles with a round shape and a size of 10 nm with a high degree of monodispersity. It was found that there was an increase of nanoparticle size with an increase of the hydrothermal process duration. The same applies to the temperature: the larger particles of the solid phase are obtained at higher temperatures [225]. Also, according to this method, particles of other morphologies can also be obtained: nanowires, nanoneedles, and nanorods with diameters of 20–150 nm and lengths of 10–300 microns [226, 227]. Thus, hydrothermal (solvothermal) synthesis is a simple, efficient, and ecological method for the chemical synthesis of metal oxides, as well as complex oxides, solid solutions, and composites [228]. In addition, the control of the main process parameters (pressure, temperature, and duration) of this method provides wide opportunities for obtaining high-quality nanoparticles of metal oxides. However, it should be noted that the method is complex in hardware design and is quite energy-consuming. Moreover, the materials used for the creation of autoclaves are subject to rigid requirements: they must be chemically inert in acid and alkaline environments at elevated temperatures and pressures.

3.1.4. Sol-Gel (Hydrolytic) Method. The sol-gel (hydrolytic) method is a universal process, which is very widely used for obtaining simple and complex metal oxides of high purity. In the typical sol-gel process, the colloidal suspension, that is, the sol, is formed by the reactions of hydrolysis and partial polymerization of precursors, which are usually inorganic metal salts or metal organic compounds, such as alcoholic metals. Full polymerization and solvent removal lead to the transition from the liquid sol to the solid gel phase. The development of nanoparticles depends on such factors as the solvent nature, pH value, solution viscosity, and

temperature. With relative simplicity and versatility of the sol-gel method, the properties of the finite material are sensitive to each stage of this process. The systematic study of the reactive parameters such as the reaction duration, temperature, concentration, and chemical composition of reagents allows controlling the size, shape, and quality of nanocrystals. Thin films of nanoparticles can be obtained by this method on the substrate area by spin-coating or dip-coating techniques [229–232]. As a result of the use of inorganic metal salts, powders with a larger particle size in comparison with the organic precursors are produced. Particles of another morphology, for example, nanofibers with an average diameter in the range of 100–300 nm and a length of more than 10 μm, can also be received by sol-gel technology.

A significant advantage of the sol-gel technology is the ability to achieve a high homogeneity of materials in the case of the synthesis of complex compounds. All precursors are in the liquid phase; their mixing is realized at the molecular level, which results in a high degree of homogeneity. Thus, it is possible to provide high-quality materials in terms of the purity, composition, and uniformity of the structure. Under certain conditions, this method can produce powders, monoliths, coatings, films, fibers, aerogels, glass, ceramics, and hybrid materials. It is also possible to synthesize both crystalline and amorphous nanopowders [233].

3.1.5. Gas Phase Synthesis Method. The gas phase synthesis method, which is based on the processes of evaporation and condensation with the passage of a chemical reaction, has recently become popular for the synthesis of metal oxide nanostructures. It is usually realized in an inert atmosphere at elevated temperatures (up to 1573 K) [234–237]. The appropriate metals and their oxides or mixtures based on them are used as precursors. This method allows receiving monocrystalline particles of various forms, such as prismatic plates, tapes, and nanowires, in diameters of 40–200 nm and in lengths from several tens to several hundreds of micrometers. In addition, this method allows obtaining monocrystals of controlled and diverse morphologies with a high degree of crystallinity [238, 239]. A feature of the CVD method is its numerous varieties, among the most popular of which is MOCVD, which is used for obtaining metal oxide powders [240].

3.1.6. Template Synthesis. Template synthesis is a process occurring under the influence of certain factors of spatial constraints—with the help of a peculiar pattern—a template that allows controlling the structure of the generated phase. Template synthesis can also be combined with methods of electrodeposition, sol-gel technology (most often), and chemical vapor deposition [241]. The method of template synthesis allows the preparation of nanoparticles of various shapes and sizes, as well as structures, for example, mesoporous structures. The disadvantages of the template method include the soft processing conditions characterized by a weak motive force of material deposition, so the process of obtaining particles by this method is quite a long-term process.

3.1.7. Electrospinning. Electrospinning is a relatively cheap and easy-to-use technology that allows synthesizing materials in the form of fibers of a certain strength and flexibility on a large scale. The method consists in the injection of precursors through stainless steel needles with the application of high voltage to produce fibrous mesh material on the collector. This technology makes it possible to obtain one-dimensional (1D) nanoscale metal oxide materials (nanofibers, nanotubes, and nanoclusters) with a required composition with the given morphology, depending on the type of the selected solvent and its viscosity, vapor pressure, and applied voltage [230, 242, 243].

3.1.8. Ecological methods. Ecological methods involve the synthesis of chemical compounds without the use of substances toxic to the environment and human health. Another advantage of such methods is their cheapness [244].

3.1.9. Green Synthesis. Green synthesis of metal oxide nanoparticles is carried out using various extracts [244, 245].

3.1.10. Combined Methods. The combination of different synthesis methods of nanoparticles allows the use of the advantages of individual methods, for example, to obtain nanocomposites with known and controlled chemical and phase composition, as well as with different and varied particle sizes [246]. Due to this, in modern practice, combined methods are gaining popularity [247]. A significant advantage of the combined methods is the possibility of obtaining both amorphous and crystalline powders with a sufficiently developed specific surface area (up to 600 m^2/g and above).

Thus, the considered methods have a high potential for obtaining nanostructured and nanodispersed metal oxides with a certain morphology and dispersion. But nowadays, the problem of the correct choice of the synthesis method of metal-oxide nanomaterials, which would allow the production of metalloxide nanomaterials with certain sorption, catalytic, surface, and structural properties, arises. In addition, it also necessary to aim to create materials with new and unique properties. This will lead to the acquisition of the newest, most effective metal-oxide nanomaterials with an ecological direction.

3.2. Creation of Nanocomposites with Metal Oxides. Certain successes have already been achieved in the synthesis of individual nanosized metal oxides, but the possibilities of synthesizing methods for the creation of nanomaterials based on the individual metal oxides, even with a certain morphology and dispersion, are limited; therefore, recently the attention of researches was focused on the creation of nanocomposites based on them. This is especially promising for nanomaterials for environmental purposes.

For example, for sorption materials a number of requirements are proposed, namely, cheapness, ease of obtaining, the possibility of reapplication, and high sorption efficiency and selectivity. It is known that one of the disadvantages of ZrO_2 as the sorbent is its high cost. To reduce the cost of such sorption materials, nanocomposites based on ZrO_2 can be created in combination with different carriers [248]. The choice of the carrier must be conditioned by

its properties, such as a developed surface, chemical inertness, and high sorption properties. The most popular carriers used today in the literature are Al_2O_3, Fe_2O_3, SiO_2, activated carbon, layered graphite, multilayer carbon nanotubes, and graphene.

The main characteristic of sorption-catalytic materials is their catalytic activity with respect to a certain list of pollutants. They should also have a large adsorption capacity in relation to the various pollutants of nature, a short time to establish the sorption equilibrium, and an ability to effectively separate from purified water to prevent a secondary contamination of the aqueous medium [3, 249, 250]. For example, TiO_2 with a particle size of about 20-30 nm will have a specific surface area of 60 m^2/g; however, after the aggregation of its particles, it can be reduced by two times or more. Obtaining nanocomposites with it and with different carriers may be one of the ways for solving this problem. As a result, the size of TiO_2 nanoparticles is stabilized on the matrix of the carrier, and the total specific surface area increases. Also, the creation and application of nanocomposites can prevent secondary contamination, and the modification of, for example, nanosized magnetite can facilitate the rapid removal of waste materials. This points to the prospect of the creation and use of nanocomposite material metal oxides.

A study on the inactivation of *Escherichia coli* shows that ZnO-TiO_2 composites exhibit high inactivation compared with ZnO and titanium (IV) oxide. The increase in the inactivation of *Escherichia coli* by ZnO-TiO_2 is explained by the separation of charge carriers in hybrid structures [251].

The analysis of literature data shows that magnetic composites based on such matrices as silica gel, activated carbon, carbon nanotubes, graphene, and clay minerals, are effective sorption materials for the extraction of heavy metals [252] and organic pollutants of a different nature [253–255]. Thus, the modification of activated carbon with a specific surface area of 430 m^2/g by nanosized magnetite results in a mesoporous composite with a specific surface area of 742 m^2/g [256], while the sorption capacities of polyethyleneimine-magnetite composites [257], silica gel-magnetite composites [258], and carbon nanotube-magnetite composites [259] containing Fe_3O_4 particles with a diameter of about 10 nm were 2-3 times higher than that of the matrix of the composites. It should be noted that the specific surface area of nanosized Fe_3O_4 is only 13 m^2/g [260].

Consequently, the advantages of creating metal oxide nanocomposites with an environmental direction can be attributed to the following factors: the ability to fix the nanodisperse state of metal oxide particles; the ability to obtain nanocomposites with certain structural-sorption characteristics and a high specific surface area; and the presence of synergistic effects in such nanocomposite materials, that is, their sorption-catalytic properties may be much better than their individual phases.

The creation of nanocomposites can be realized in different ways. In the literature, the most promising ways of creation are considered to be [3] the intercalation of nanosized particles in the porous system, deposition of nanosized particles on the inner pore surface of various rigid matrices (polymers, zeolites, and carbon materials), obtaining hybrid materials by sol-gel methods, etc.

The structures of some nanocomposites with metal oxides obtained in laboratory conditions are shown in Figure 15. As can be seen from Figure 15, the structure of composite materials can vary considerably: it is possible to obtain the numerical number of nanocomposites that will have various physical and chemical properties by varying the ratio of components, the nature of the matrix, and the synthesis method.

Proceeding from this, it can be argued that the nanocomposite era has only begun. Also, there is no information in modern literature regarding the influence of certain parameters on the final properties of composites for environmental purposes, but only a few studies with some of their types are available. Thus, carrying out systematic and comprehensive research on the synthesis and detection of the physicochemical properties of nanocomposite materials with metal oxides is the urgent and relevant issue that will allow the development of the scientific basis for the creation and use of the newest nanocomposites based on metal oxides for environmental purposes in order to improve their sorption and (photo)catalytic characteristics in comparison with the metal oxide counterparts.

4. Features of the Use of Metal Oxides and Nanocomposites Based on Them for Ecological Purposes

4.1. Nanomaterials Based on Pure Metal Oxides. As shown above, nanomaterials based on nanostructured and nanodispersed metal oxides are characterized by valuable electrical, optical, and magnetic properties. In view of this, they are used more and more in applied ecology, especially as adsorbents and photocatalysts, as well as materials used for the manufacture of environmental monitoring devices.

Adsorption materials based on nanosized metal oxides should have a large specific surface area, high capacity, fast kinetics, and specific affinity for various contaminants [3, 249, 250]. The use of nanostructured metal oxides in photocatalytic processes can permit the oxidation of organic compounds that are not decomposed biochemically, and the treatment of aqueous solutions by their use is considered to be the most promising [250]. Metalloxide nanostructures used in environmental monitoring as sensitive layers of chemoresistive gas sensors are characterized by high values of the sensory signal due to the significant specific surface area; hence, the higher adsorption capacity [8]. Consequently, nanosized metal oxide materials are of considerable interest because of their significant advantages over bulk analogues and because of the great prospects for obtaining new types of adsorbents, photocatalysts, and sensitive layers of gas sensors based on them.

Nowadays materials based on nanodispersed TiO_2 have the greatest demand as photocatalysts and disinfectants. Titanium (IV) oxide-based sorbents and photocatalysts are particularly effective in extracting a wide range of pollutants

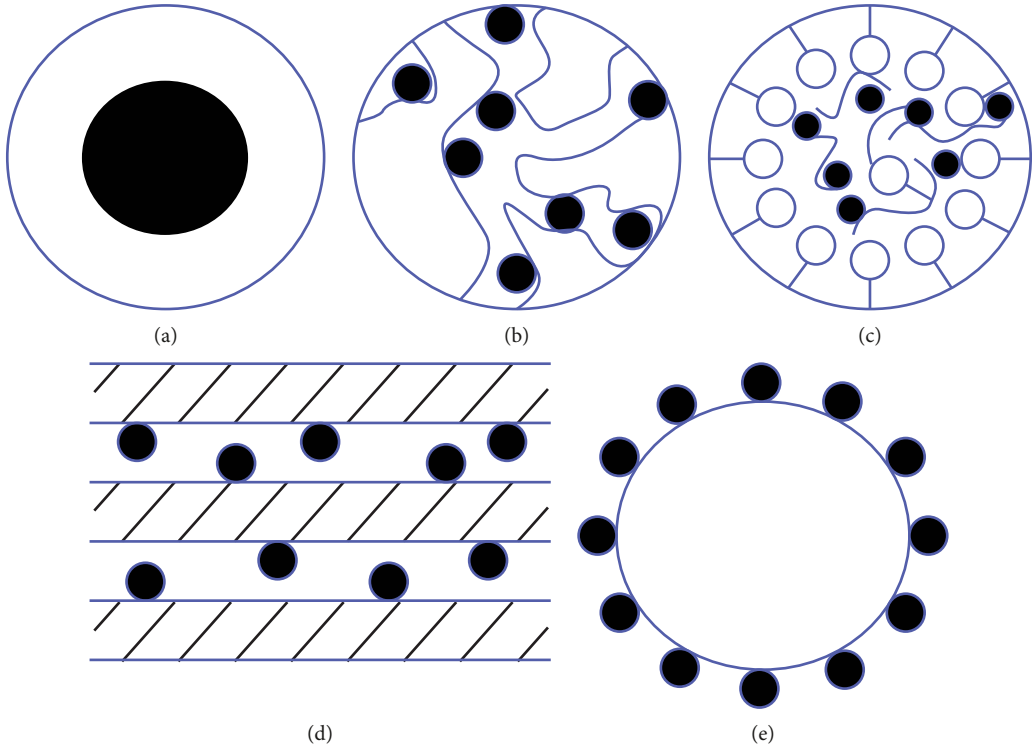

Figure 15: Nanocomposites based on nanodispersed metal oxides for environmental applications [261]: (a) core-shell structure; (b) with carbon materials and (c) with polymers; (d) surface modification of clay minerals and (e) nonporous metal oxide particles.

from water systems [262, 263]. This is evidenced by the growing number of researches devoted to this topic in the world. The mechanisms of photocatalysis involving metal oxides are presented in many studies [264–273]. At the same time, the prospects of using 1D nanostructures for photocatalytic processes, which have better transport characteristics than traditional nanoparticles, have recently been noted [274, 275].

However, unfortunately, these nanomaterials still do not have a commercial application because of their tendency to agglomerate due to the Van der Waal forces or other interactions [276], which results in a significant reduction or even the loss of the high adsorption capacity and selectivity with prolonged use. In addition, the disadvantages that limit the practical use of titanium (IV) oxide as a photocatalyst also include the high band gap, high recombination rate of electron-hole pairs, and low efficiency of the photocarrier separation [277]. It is known that the absorption of photons by particles of titanium (IV) oxide occurs only if the photon energy is greater than the energy of the forbidden band. In the case of the TiO_2 anatase modification, its surface photoactivation can be carried out exclusively under the influence of ultraviolet radiation (≤390 nm). However, only by 5% of sunlight consists of ultraviolet light (300-400 nm); therefore, the use of sunlight for the photoactivation of the pure anatase phase is not promising. The high recombination rate of the electron-hole pairs leads to the decrease in the photocatalytic efficiency of TiO_2 and, as a consequence, to the low quantum yield rate and limited photooxidation rate. The low efficiency of the photocarrier separation leads to the recombination, and therefore, to the low photocatalytic activity of photocatalysts.

One of the ways to improve the photocatalytic properties of TiO_2 is by doping or by modifying [277, 278]. This is achieved by self-doping, doping with nonmetals, doping with transition and rare-earth metals, or modifying with noble metals. As a result, the adsorption capacity and photocatalytic activity are improved. Using doping, additional energy levels are created in the structure of the zones that can be used to trap electrons or holes. As a result, the carriers are separated, which allows them to diffuse to the surface successfully. Also, as a result of doping, the desired redshift of the absorption edge can be achieved. Thus, doping can change both the electronic structure and the band gap, which ultimately leads to the optimization of the optical properties and the reduction of the massive recombination of photogenerated carriers in TiO_2. In addition, as was shown previously, the photocatalytic activity strongly depends on the set of open crystal facets, which have different levels of surface energy for the conduction band (CB) and valence band (VB), which can affect the carrier transport. The facet structure of TiO_2 particles can also be effectively modified by doping [264].

In addition to doping, for the change in the electronic properties of photocatalysts based on titanium (IV) oxide the method of ionic implantation of metals was proposed in [279], which resulted in photocatalysts that effectively absorb and work not only under ultraviolet light, but also under visible radiation (even longer than 550 nm). This, according to the authors, can be the important breakthrough in the use

of safe sunlight energy, which can shift these researches into the field of sustainable green chemistry.

In order to reduce the rate of recombination or even prevent it, the creation (excluding modifying) of nanocomposites based on titanium (IV) oxide is proposed [278, 280]. The modification of titanium (IV) oxide with noble metals (Au, Ag, Pt, and Pd) effectively increases the photocatalytic efficiency of TiO_2, but it is a very expensive process. In this composite, the metal plays a dual role as a catalyst and trap for electrons. Metal nanoparticles direct flows of photoinduced electrons and holes in opposite directions, which prevents their recombination [277]. Combining two semiconductors with the corresponding potentials of the conduction band and the valence band are considered to be a promising direction for increasing photocatalytic activity.

In recent years, a number of studies have been carried out on the formation of TiO_2-based heterostructures in conjunction with other semiconductors such as SnO_2, WO_3, Fe_2O_3, ZnO, and CdS, among which TiO_2 and SnO_2 composites are the most noteworthy. Nanocomposites of the TiO_2-SnO_2 anatase-rutile modification are characterized by the highest levels of photocatalytic activity due to the effects of the merging of SnO_2 nanoparticles and the coexistence of the phases of anatase and rutile [281, 282]. In addition, titanium (IV) oxide and tin (IV) oxide have similar ion radii (0.68 Å for Ti^{4+} and 0.71 Å for Sn^{4+}) and have similar structural (tetragonal structure of the rutile type) and electronic properties. The band gap widths of SnO_2, TiO_2 (anatase), and TiO_2(rutile) are 3.6 eV, 3.2 eV, and 3.0 eV, respectively, and the potential of the conduction band of tin (IV) oxide is approximately 0.5 V more positive than that of titanium (IV) oxide [281].

The use of ZnO-based photocatalysts for photooxidative degradation of organic pollutants in aqueous solutions looks promising and may be a good alternative of using TiO_2-based photocatalysts [283]. Its advantages include high potential efficiency, relative cheapness, high stability, nontoxicity, the absence of secondary pollution, and the possibility of decomposing harmful organic pollutants into less harmful pollutants in a relatively short time [284].

Photocatalysts based on zinc oxide synthesized by the sol-gel method show a high degree of removal (99.7%) of anionic dyes (for example, methylene orange) from aqueous solutions. The resulting photocatalyst efficiently and quickly decomposes azo dyes by the generated superoxide ions, which were the main species [285]. ZnO nanoparticles, which were obtained by the hydrothermal method, had various nanostructures, depending on the pH: nanorods, hexagonal disks, porous nanorods, and nanoflower structures. The photocatalytic activity of the obtained ZnO nanoparticles, estimated by the dye rhodamine B (RhB), was not lower than 94%. The photocatalyst had good stability for five cycles [286]. Thus, zinc oxide is an economical and environmentally friendly photocatalyst that can be used to clean wastewater contaminated with synthetic dyes.

It should be noted that photocatalysis with both TiO_2 and ZnO depends on the structural design of their particles, which are classified according to a known dimensional classification. In a zero-dimensional structure in the form of spheres, these materials have a high specific surface area and a porous structure. One-dimensional structures such as fibers or tubes may have lower recombination levels. Two-dimensional structures of titanium (IV) oxide and zinc oxide are characterized by a flat surface, high compression ratio, low turbidity, and excellent adhesion to substrates; as a result, they can be effectively used in self-cleaning glasses. The three-dimensional architectures of these materials can provide potential benefits for cleaning, separation, and storage. In general, the properties of these materials strongly depend on the dimensions of their structures; therefore, it is very important that the dimensions are taken into account before their use [287].

Despite the rather significant advantages, the use of photocatalysts based on ZnO has some problems: ZnO does not absorb the visible part of the solar spectrum and requires costly ultraviolet radiation to excite charge carriers that can recombine quickly; it is difficult to extract ZnO powder from the suspension after the photocatalytic process; ZnO has a tendency to aggregate during photocatalysis; and, most importantly, ZnO is susceptible to corrosion under the influence of ultraviolet light [111].

All these suggests that oxidative methods can solve the problem of the lack of clean water [288]. Directional modification or doping, creating the specific morphology and architecture, and attaining the required degree of crystallinity and the highest specific surface area are necessary for effective photocatalyst usage; creating metal oxide nanocomposites also looks very promising. The synthesis and characterization of porous ZnO-SnO_2 nanosheets obtained by the hydrothermal method in [289] showed the well-crystallized, porous, and well-defined morphology of the nanosheet material. The synthesized ZnO-SnO_2 nanocomposites were used as an effective photocatalyst and as a material in the manufacture of a chemical sensor. The photocatalytic degradation of the highly dangerous dye, direct blue 15, was carried out under irradiation with visible light. The synthesized nanocomposites were also used for the detection of 4-nitrophenol in an aqueous medium. The synthesized nanocomposites were highly active and highly sensitive. According to the authors, the obtained result was due to the formation of a ZnO-SnO_2 heterojunction, which effectively separates the photogenerated electron-hole pairs, and the high surface area.

The successful use of nanomaterials based on zinc oxide in electrochemical sensors is due to such properties as high specific surface area, chemical and photochemical stability, nontoxicity, electrochemical activity, and ease of synthesis. Its electrochemical activity and electronic communication features make it possible to consider ZnO-based nanomaterials as excellent candidates for electrochemical sensors [290]. However, the elevated operating temperature is still the bottleneck of widespread ZnO usage in real-time gas monitoring; thus, research to reduce the operating temperature is currently underway. To overcome this difficulty, surface modification, doping, and light activation are mainly proposed [291].

SnO_2-based nanostructures are already widely used in the creation of miniature chemoresistive gas sensors with

minimal energy consumption and high sensitivity [292]. However, the sensitivity and selectivity of SnO_2 sensors still remain as pressing questions. To increase the sensitivity of SnO_2-based nanostructures, a modification with various activating additives is necessary. Increasing the selectivity can be achieved by creating appropriate nanocomposites and obtaining information from several sensitive layers simultaneously with its subsequent mathematical processing. In this case, SnO_2-based nanostructures can be used to detect the most diverse components in the gas mixture, such as acetone, NH_3, NO_x, SO_2, H_2, CH_4, CO, CO_2, LPG, and others [293, 294].

Nanomaterials based on ZrO_2 are characterized by sufficiently high catalytic activity and sorption capacity due to the significant specific surface area of nanodispersed ZrO_2. Inorganic ion exchangers and adsorbents with ZrO_2 have certain advantages over known organic resins, since they are chemically stable even under high temperature [295]. The only drawback of sorption materials based on nanodispersed ZrO_2 is their relatively high cost.

For ecological purposes, all crystalline modifications of ZrO_2, as well as its amphoteric form, are used. Amphoteric zirconium (IV) oxide behaves as the anion exchange resin in an acidic and neutral solution and as the cation resin in an alkaline solution. The value of amphoteric ZrO_2 is that it can be successfully used in the processing of radioactive waste [296–298].

Crystalline ZrO_2 is an important material and is widely used in ceramic technology and in heterogeneous catalysis. Due to the nature of the n-type semiconductor, it has recently been considered as a photocatalyst in photochemical heterogeneous reactions. The report in the scientific literature of the energy values of the forbidden zone in the range from 3.25 to 5.1 eV, depending on the method of sample preparation, also contributed to this [299]. It is reported that nanoscale ZrO_2 of all modifications (monoclinic, tetragonal, and cubic) can be used as photocatalysts. In [300], ZrO_2 was studied as the catalyst for the photocatalytic degradation of methyl orange and the effect of all modifications was shown. It was found that the photocatalytic activity of the pure monoclinic ZrO_2 sample is higher than that of the tetragonal and cubic ZrO_2 samples under identical conditions. The authors explain the higher activity of the monoclinic ZrO_2 sample with respect to the photocatalytic degradation of methyl orange by the presence of a small amount of the oxygen-deficient zirconium oxide phase, high crystallinity, large pores, and the high density of surface hydroxyl groups.

In recent years, intensive research for the synthesis and use of nanoparticles based on ferric oxide, especially magnetite, which has magnetic properties that can be varied in a wide range due to the change in size and morphology, has begun. High surface-to-volume ratio and superparamagnetism make these ferromagnetic nanoparticles particularly attractive for use in the ecological direction [301]. In addition, magnetite nanoparticles are nontoxic, chemically inert, and biocompatible; therefore, they also have a huge potential for use in water purification.

The applications of nanoparticles based on TiO_2, ZnO, SnO_2, ZrO_2, and Fe_3O_4 in the ecological direction listed here indicate the likely prospect of creating new environmental technologies with their participation.

4.2. Nanocomposite Metal Oxide Materials. In modern literature, more and more studies on the creation of metal-oxide nanocomposites, an extremely promising type of nanomaterial, appear. Because of their structure, nanocomposites have specific, sometimes unique, physical and chemical properties and can be applied in a wide variety of fields, including engineering, medicine, and ecology as well as in the production of new materials in the construction industry.

Obtaining nanocomposites with metal oxides for water purification is considered in terms of stabilizing the latter in the matrix of the composite and their easy separation after the completion of the processes of sorption and photocatalysis. In addition, the use of individual nanodispersed metal oxides can lead to environmental contamination with nanoparticles but using them as part of nanocomposites will prevent this [3]. Nanocomposites based on nanodispersed oxides of titanium and zirconium and a carbon matrix (activated carbon, carbon nanotubes, and graphene) indeed have great potential for use in water purification [302]. Mesoporous oxides of titanium and zirconium are characterized by high values of exchange capacity and chemical and thermal resistance, and carbon materials have mechanical strength, resistance to aggressive environments, and a well-developed porous structure. It is possible to obtain fundamentally new sorption materials that will have this given set of properties by combining these phases.

In assessing the promising use of metal oxide nanocomposites based on activated carbon for sorption and photocatalytic purposes, it was noted that the increase of the sorption capacity and photocatalytic activity of organic substances is at least 2.5 times compared with those of pure metal oxides [303]. The introduction, for example, of TiO_2 in a matrix with a diverse nature increases not only the adsorption capacity but also the chemical stability of the final composite material [304].

ZnO-based nanocomposites for environmental applications are becoming increasingly popular. The most diverse composites are synthesized based on it, where both natural substances (clay minerals, chitin, and chitosan) and artificial ones (graphene, CNT, polymers, and other metal oxides) are used as a matrix [305, 306].

The creation of composites based on zinc oxide, for example, ZnO-graphene, allows obtaining photocatalytically active catalysts with respect to antibiotics in wastewater [307]. The obtained ZnO-reduced graphene oxide (rGO) nanocomposites in [308] showed more than doubled photocatalytic activity in visible light to dyes of different natures compared to pure ZnO. The photoactivity of nanocomposites is due to the smaller size of ZnO nanorods and the presence of rGO, which acts as the photosensitizer, transferring electrons to the ZnO conduction band inside the nanocomposite when illuminated by sunlight.

Obtaining mixed oxide nanocomposites with the participation of various oxides is considered very promising for the creation of effective photocatalysts/sorbents to organic pollutants. This fact is confirmed by the authors in [309], who

showed that the mixed oxide nanocomposite WO_3-ZnO is the most effective photocatalyst for the decomposition of organic pollutants in water compared to commercial ZnO.

It was established that the creation of nanocomposites based on tin (IV) oxide with other metal oxides for their usage as sensitive layers of gas sensors can increase the selectivity of the detection of certain analytes. At the same time, due to the developed surface of metal oxides and the low solubility of metal oxide additives in them, there is mainly the superficial distribution of modifiers. This leads to the purposeful change in the surface state and the creation of additional active centers, contributing to the separation of the functions of the metal oxide surface (receptor) and volume (converter) [310]. SnO_2-carbon nanotube nanocomposites exhibit high sensitivity at low power consumption; therefore, effective devices for monitoring the environment at ambient temperatures can be created based on such compositions [311–313].

For the "zirconium (IV) oxide-activated carbon nanocomposite," a synergistic effect in extracting heavy metals from aqueous solutions was found (the sorption capacity of the nanocomposite, for example, was 8 times higher than that of pure ZrO_2 and 3.15 times higher than that of activated carbon) [227]. Even the ordinary mixing of nanosized titanium oxide with activated carbon leads to the increase in the sorption capacity by 1.3 times [314].

In recent years, the development of nanocomposite magnetic sorbent materials based on minerals is also growing due to the possibility of the easy removal of clay minerals after the completion of the sorption process. The synthesis of magnetite-containing particles and their modification are considered "green" technologies, and the sorbents themselves are "green" materials [315–318], while the creation of magnetic sorbents is already offered from a variety of wastes [319]. According to the results of the studies, the modification of a clay matrix such as zeolites, bentonites, and montmorillonite clays by nanosized magnetite does not reduce the adsorption capacity [320, 321], and in some cases even increases it [124, 254].

The analysis of the relevant literary sources leads to the conclusion that studies devoted to the synthesis and use of nanocomposite metal oxide materials in the ecological direction are almost not carried out. Therefore, today this is the rather topical issue, the solution of which will lead to the creation of new technologies for obtaining and using composite nanomaterials in the recovery of the environment and catalysis.

5. Conclusions

The considered features of the properties and the creation of metal oxide nanomaterials and nanocomposites based on TiO_2, ZnO, SnO_2, ZrO_2, and Fe_3O_4 for ecological applications show the likely prospect of the development of this scientific and practical direction. It is shown that the dispersion and morphology of nanoparticles have a determining influence on the finite physical and chemical characteristics of metal oxide nanomaterials. For TiO_2, ZnO, SnO_2, ZrO_2, and Fe_3O_4, the crystallochemical characteristic, the surface structure, and the features of surface phenomena, which have a significant effect on their sorption and catalytic properties, are given. Their use as sorbents, photocatalysts, and sensitive layers of gas sensors has been substantiated. It is shown that the creation of metal-oxide composite nanomaterials, which will have better sorption and catalytic properties than their individual metal oxide nanomaterials due to the synergistic effects and special structural and adsorption characteristics, is the most promising direction. This will allow obtaining a fundamentally new class of nanomaterials for environmental purposes. Based on the analysis of modern literary sources, it is expected that the use of metal-oxide nanocomposites for environmental applications will lead to the development of new effective environmentally and economically feasible technologies.

Conflicts of Interest

The authors declare that there is no conflict of interest regarding the publication of this paper.

Acknowledgments

The authors thank the Faculty of Chemical Technology of the National Technical University of Ukraine "Igor Sikorsky Kyiv Polytechnic Institute" for support in conducting this research. The authors also thank the Postgraduate and Doctoral Studies Department of the National Technical University of Ukraine "Igor Sikorsky Kyiv Polytechnic Institute" for funding support.

References

[1] J. L. G. Fierro, Ed., *Metal Oxides: Chemistry and Application*, Taylor & Francis, CRC Press, 2006.

[2] S. R. Kumar and P. Gopinath, *Nano-Bioremediation Applications of Nanotechnology for Bioremediation*, in The Book: Remediation of Heavy Metals in the Environment, CRC Press, Boca Raton, 2016.

[3] Y. Zhang, B. Wu, H. Xu et al., "Nanomaterials-enabled water and wastewater treatment," *NanoImpact*, vol. 3-4, pp. 22–39, 2016.

[4] C. Santhosh, V. Velmurugan, G. Jacob, S. K. Jeong, A. N. Grace, and A. Bhatnagar, "Role of nanomaterials in water treatment applications: a review," *Chemical Engineering Journal*, vol. 306, pp. 1116–1137, 2016.

[5] A. A. Werkneh and E. R. Renein, *Applications of Nanotechnology and Biotechnology for Sustainable Water and Wastewater Treatment*, in The Book: Water and Wastewater Treatment Technologies, Energy, Environment, and Sustainability, Springer, Singapore, 2019.

[6] M. Cerro-Lopez and M. A. Méndez-Rojas, "Application of nanomaterials for treatment of wastewater containing pharmaceuticals," in *The Handbook of Environmental Chemistry*, vol. 66, Springer, Cham, 2017.

[7] M. Pelaez, N. T. Nolan, S. C. Pillai et al., "A review on the visible light active titanium dioxide photocatalysts for environmental applications," *Applied Catalysis B: Environmental*, vol. 125, no. 21, pp. 331–349, 2012.

[8] C. Xu, J. Tamaki, N. Miura, and N. Yamazoe, "Grain size effects on gas sensitivity of porous SnO_2-based elements," *Sensors and Actuators B: Chemical*, vol. 3, no. 2, pp. 147–155, 1991.

[9] D. R. Miller, S. A. Akbar, and P. A. Morris, "Nanoscale metal oxide-based heterojunctions for gas sensing: a review," *Sensors and Actuators B: Chemical*, vol. 204, pp. 250–272, 2014.

[10] T. A. Miller, S. D. Bakrania, C. Perez, and M. S. Wooldridge, "Nanostructured tin dioxide materials for gas sensor applications," *Functional Nanomaterials*, vol. 30, pp. 1–24, 2006.

[11] U. Diebold, "The surface science of titanium dioxide," *Surface Science Reports*, vol. 48, no. 5-8, pp. 53–229, 2003.

[12] S. M. Gupta and M. Tripathi, "A review of TiO_2 nanoparticles," *Chinese Science Bulletin*, vol. 56, no. 16, pp. 1639–1657, 2011.

[13] A. S. Barnard and P. Zapol, "Effects of particle morphology and surface hydrogenation on the phase stability of TiO_2," *Physical Review B*, vol. 70, no. 23, article 235403, p. 23, 2004.

[14] H. Morkoç and Ü. Özgür, *Zinc Oxide: Fundamentals, Materials and Device Technology*, Wiley-VCH Verlag GmbH & Co. KGaA, 2009.

[15] M. I. H. Chowdhury, M. S. Hossain, M. A. S. Azad, M. Z. Islam, and M. A. Dewan, "ZnO: material, physics and applications," *Chemphyschem*, vol. 8, no. 6, pp. 782–803, 2007.

[16] M. A. Maki-Jaskari and T. T. Rantala, "Band structure and optical parameters of the SnO_2(110) surface," *Physical Review B*, vol. 64, no. 7, article 075407, 2001.

[17] H. K. Shashikumar, M. Siddaraju, and B. N. Chethan, "Structure simulation and study of electronic and dielectric properties of tin dioxide," *Inorganic Chemistry: An Indian Journal*, vol. 10, no. 4, pp. 148–151, 2015.

[18] I. D. Muhammad, M. Awang, O. Mamat, and Z. B. Shaari, "First-principles calculations of the structural, mechanical and thermodynamics properties of cubic zirconia," *World Journal of Nano Science and Engineering*, vol. 4, no. 2, pp. 97–103, 2014.

[19] S. Banerjee and P. Mukhopadhyay, *Phase Transformations: Examples from Titanium and Zirconium Alloys*, Elsevier Ltd., 2007.

[20] R. J. Nicholls, N. Ni, S. Lozano-Perez et al., "Crystal structure of the ZrO_2 phase at zirconium/zirconium oxide interfaces," *Advanced Engineering Materials*, vol. 17, no. 2, pp. 211–215, 2015.

[21] I. Nettleship and R. Stevens, "Tetragonal zirconia polycrystal (TZP)—a review," *International Journal of High Technology Ceramics*, vol. 3, no. 1, pp. 1–32, 1987.

[22] G. Dercz, K. Prusik, and L. Pajak, "X-ray and SEM studies on zirconia powders," *Journal of Achievements in Materials and Manufacturing Engineering*, vol. 31, no. 2, pp. 408–414, 2008.

[23] G. S. Parkinson, "Iron oxide surfaces," *Surface Science Reports*, vol. 71, no. 1, pp. 272–365, 2016.

[24] K. E. Sickafus, J. M. Wills, and N. W. Grimes, "Structure of spinel," *Journal of the American Ceramic Society*, vol. 82, no. 12, pp. 3279–3292, 1999.

[25] A. W. Adamson and A. P. Gast, *Physical Chemistry of Surfaces*, Wiley-Interscience, New York, NY, USA, 6th edition, 1997.

[26] M. Ramamoorthy, R. D. King-Smith, and D. Vanderbilt, "Defects on TiO_2 (110) surfaces," *Physical Review B*, vol. 49, no. 11, pp. 7709–7715, 1994.

[27] W. C. Mackrodt, E. A. Simson, and N. M. Harrison, "An ab initio Hartree-Fock study of the electron-excess gap states in oxygen-deficient rutile TiO_2," *Surface Science*, vol. 384, no. 1–3, pp. 192–200, 1997.

[28] A. Vijay, G. Mills, and H. Metiu, "Adsorption of gold on stochiometric and reduced rutile TiO_2 (110) surfaces," *The Journal of Chemical Physics*, vol. 118, no. 14, pp. 6536–6551, 2003.

[29] J. Oviedo, M. A. San Miguel, and J. F. Sanz, "Oxygen vacancies on TiO_2 (110) from first-principles calculations," *The Journal of Chemical Physics*, vol. 121, no. 15, pp. 7427–7433, 2004.

[30] M. Menetrey, A. Markovits, and C. Minot, "Reactivity of a reduced metal oxide surface: hydrogen, water and carbon monoxide adsorption on oxygen defective rutile TiO_2(110)," *Surface Science*, vol. 524, no. 1–3, pp. 49–62, 2003.

[31] A. T. Paxton and L. Thien-Nga, "Electronic structure of reduced titanium dioxide," *Physical Review B*, vol. 57, no. 3, pp. 1579–1584, 1998.

[32] P. J. D. Lindan, N. M. Harrison, M. J. Gillan, and J. A. White, "First-principles spin-polarized calculations on the reduced and reconstructed TiO_2 (110) surface," *Physical Review B*, vol. 55, no. 23, pp. 15919–15927, 1997.

[33] M. D. Rasmussen, L. M. Molina, and B. Hammer, "Adsorption, diffusion and dissociation of molecular oxygen at defected TiO_2(110): a density functional theory study," *The Journal of Chemical Physics*, vol. 120, no. 2, pp. 988–997, 2004.

[34] X. Wu, A. Selloni, and S. K. Nayak, "First principles study of CO oxidation on TiO_2 (110): the role of surface oxygen vacancies," *The Journal of Chemical Physics*, vol. 120, no. 9, pp. 4512–4516, 2004.

[35] X. Wu, A. Selloni, M. Lazzeri, and S. K. Nayak, "Oxygen vacancy mediated adsorption and reactions of molecular oxygen on the TiO_2(110) surface," *Physical Review B*, vol. 68, no. 24, article 241402, 2003.

[36] A. Vittadini and A. Selloni, "Small gold clusters on stochiometric and defected TiO_2 anatase (101) and their interaction with CO: a density functional study," *The Journal of Chemical Physics*, vol. 117, no. 1, pp. 353–361, 2002.

[37] Y.-F. Zhang, W. Lin, Y. Li, K. N. Ding, and J. Q. Li, "A theoretical study on the electronic structures of TiO_2: effect of Hartree-Fock exchange," *The Journal of Physical Chemistry B*, vol. 109, no. 41, pp. 19270–19277, 2005.

[38] C. Di Valentin, G. Pacchioni, and A. Selloni, "Electronic structure of defect states in hydroxylated and reduced rutile TiO_2 (110) surfaces," *Physical Review Letters*, vol. 97, no. 16, article 166803, 2006.

[39] E. Cho, S. Han, H.-S. Ahn, K. R. Lee, S. K. Kim, and C. S. Hwang, "First-principles study of defects in rutile TiO_{2-x}," *Physical Review B*, vol. 73, no. 19, article 193202, 2006.

[40] C. di Valentin, G. Pacchioni, and A. Selloni, "Theory of carbon doping of titanium dioxide," *Chemistry of Materials*, vol. 17, no. 26, pp. 6656–6665, 2005.

[41] K. Hameeuw, G. Cantele, D. Ninno, F. Trani, and G. Iadonisi, "Influence of surface and subsurface defects on the behavior of the rutile TiO_2 (110) surface," *Physica Status Solidi (A)*, vol. 203, no. 9, pp. 2219–2222, 2006.

[42] M. V. Ganduglia-Pirovano, A. Hofmann, and J. Sauer, "Oxygen vacancies in transition metal and rare earth oxides: current state of understanding and remaining challenges," *Surface Science Reports*, vol. 62, no. 6, pp. 219–270, 2007.

[43] M. Ramamoorthy, D. Vanderbilt, and R. D. King-Smith, "First-principles calculations of the energetics of stoichiometric TiO_2 surfaces," *Physical Review B*, vol. 49, no. 23, pp. 16721–16727, 1994.

[44] S. Andersson, B. Collén, U. Kuylenstierna et al., "Phase analysis studies on the titanium-oxygen system," *Acta Chemica Scandinavica*, vol. 11, pp. 1641–1652, 1957.

[45] J. B. Goodenough, "Metallic oxides," *Progress in Solid State Chemistry*, vol. 5, pp. 145–399, 1972.

[46] Z. Zhang and J. T. Yates, *Defects on TiO_2-Key Pathways to Important Surface Processes*, in The Book: Defects at Oxide Surfaces, Springer, Switzerland, 2015.

[47] M. Lazzeri, A. Vittadini, and A. Selloni, "Structure and energetics of stochiometric TiO_2 anatase surfaces," *Physical Review B*, vol. 63, no. 15, article 155409, 2001.

[48] U. Diebold, N. Ruzycki, G. S. Herman, and A. Selloni, "One step towards bridging the materials gap: surface studies of TiO_2 anatase," *Catalysis Today*, vol. 85, no. 2–4, pp. 93–100, 2003.

[49] D. J. Cooke, A. Marmier, and S. C. Parker, "Surface structure of $(10\bar{1}0)$ and $(11\bar{2}0)$ surfaces of ZnO with density functional theory and atomistic simulation," *The Journal of Physical Chemistry B*, vol. 110, no. 15, pp. 7985–7991, 2006.

[50] A. Janotti and C. G. van de Walle, "Fundamentals of zinc oxide as a semiconductor," *Reports on Progress in Physics*, vol. 72, no. 12, article 126501, 2009.

[51] M. A. Maki-Jaskari and T. T. Rantala, "Theoretical study of oxygen-deficient SnO_2 (110) surfaces," *Physical Review B*, vol. 65, no. 24, article 245428, 2002.

[52] T. T. Rantala, T. S. Rantala, and V. Lantto, "Surface relaxation of the (110) face of rutile SnO_2," *Surface Science*, vol. 420, no. 1, pp. 103–109, 1999.

[53] T. T. Rantala, T. S. Rantala, and V. Lantto, "Electronic structure of SnO_2 (110) surface," *Materials Science in Semiconductor Processing*, vol. 3, no. 1–2, pp. 103–107, 2000.

[54] A. Bouzoubaa, A. Markovits, M. Calatayud, and C. Minot, "Comparison of the reduction of metal oxide surfaces: TiO_2-anatase, TiO_2-rutile and SnO_2-rutile," *Surface Science*, vol. 583, no. 1, pp. 107–117, 2005.

[55] E. A. Florianoa, L. V. A. Scalvia, J. R. Sambranoc, and V. Geraldo, "Evaluation of bulk and surfaces absorption edge energy of sol-gel-dip-coating SnO_2 Thin Films," *Materials Research*, vol. 13, no. 4, pp. 437–443, 2010.

[56] I. Manassidis, J. Goniakowski, L. N. Kantorovich, and M. J. Gillan, "The structure of the stoichiometric and reduced SnO_2 (110) surface," *Surface Science*, vol. 339, no. 3, pp. 258–271, 1995.

[57] D. F. Cox, T. B. Fryberger, and S. Semancik, "Oxygen vacancies and defect electronic states on the SnO_2 (110)-1×1 surface," *Physical Review B*, vol. 38, no. 3, pp. 2072–2083, 1988.

[58] M. Sinner-Hettenbach, M. Göthelid, J. Weissenrieder et al., "Oxygen-deficient SnO_2 (110): a STM, LEED and XPS study," *Surface Science*, vol. 477, no. 1, pp. 50–58, 2001.

[59] J. M. Themlin, R. Sporken, J. Darville, R. Caudano, J. M. Gilles, and R. L. Johnson, "Resonant-photoemission study of SnO_2: cationic origin of the defect band-gap states," *Physical Review B*, vol. 42, no. 18, pp. 11914–11925, 1990.

[60] M. Sinner-Hettenbach, M. Göthelid, T. Weiß et al., "Electronic structure of SnO_2 (110)-4×1 and sputtered SnO_2 (110) revealed by resonant photoemission," *Surface Science*, vol. 499, no. 1, pp. 85–93, 2002.

[61] J. Oviedo and M. J. Gillan, "The energetics and structure of oxygen vacancies on the SnO_2 (110) surface," *Surface Science*, vol. 467, no. 1–3, pp. 35–48, 2000.

[62] J. Oviedo and M. J. Gillan, "Reconstructions of strongly reduced SnO_2 (110) studied by first-principles methods," *Surface Science*, vol. 513, no. 1, pp. 26–36, 2002.

[63] R. G. Egdell, S. Eriksen, and W. R. Flavell, "Oxygen deficient SnO_2 (110) and TiO_2 (110): a comparative study by photoemission," *Solid State Communications*, vol. 60, no. 10, pp. 835–838, 1986.

[64] D. F. Cox, S. Semancik, and P. D. Szuromi, "Structural and electronic-properties of clean and water dosed SnO_2 (110)," *Journal of Vacuum Science & Technology A*, vol. 4, no. 3, pp. 627-628, 1986.

[65] D. F. Cox, T. B. Fryberger, J. W. Erickson, and S. Semancik, "Surface-properties of clean and gas-dosed SnO_2 (110)," *Journal of Vacuum Science & Technology A*, vol. 5, no. 4, pp. 1170-1171, 1987.

[66] E. de Frésart, J. Darville, and J. M. Gilles, "Influence of the surface reconstruction on the work function and surface conductance of (110) SnO_2," *Applications of Surface Science*, vol. 11-12, pp. 637–651, 1982.

[67] D. F. Cox and T. B. Fryberger, "Preferential isotopic labeling of lattice oxygen positions on the SnO_2 (110) surface," *Surface Science*, vol. 227, no. 1–2, pp. L105–L108, 1990.

[68] A. Atrei, E. Zanazzi, U. Bardi, and G. Rovida, "The SnO_2 (110) (4×1) structure determined by LEED intensity analysis," *Surface Science*, vol. 475, no. 1–3, pp. L223–L228, 2001.

[69] F. H. Jones, R. Dixon, J. S. Foord, R. G. Egdell, and J. B. Pethica, "The surface structure of SnO_2 (110) (4×1) revealed by scanning tunneling microscopy," *Surface Science*, vol. 376, no. 1–3, pp. 367–373, 1997.

[70] C. L. Pang, S. A. Haycock, H. Raza, P. J. Møller, and G. Thornton, "Structures of the 4×1 and 1×2 reconstructions of SnO_2 (110)," *Physical Review B*, vol. 62, no. 12, pp. R7775–R7778, 2000.

[71] M. Batzill, K. Katsiev, J. M. Burst, U. Diebold, A. M. Chaka, and B. Delley, "Gas-phase-dependent properties of SnO_2 (110), (100), and (101) single-crystal surfaces: structure, composition, and electronic properties," *Physical Review B*, vol. 72, no. 16, article 165414, 2005.

[72] M. Batzill, A. M. Chaka, and U. Diebold, "Surface oxygen chemistry of a gas-sensing material: SnO_2(101)," *Europhysics Letters*, vol. 65, no. 1, pp. 61–67, 2004.

[73] M. Batzill and U. Diebold, "The surface and materials science of tin oxide," *Progress in Surface Science*, vol. 79, no. 2-4, pp. 47–154, 2005.

[74] M. Batzill and U. Diebold, "Characterizing solid state gas responses using surface charging in photoemission: water adsorption on SnO_2(101)," *Journal of Physics: Condensed Matter*, vol. 18, no. 8, pp. L129–L134, 2006.

[75] M. Batzill, K. Katsiev, J. M. Burst et al., "Tuning surface properties of SnO_2 (101) by reduction," *Journal of Physics and Chemistry of Solids*, vol. 67, no. 9–10, pp. 1923–1929, 2006.

[76] M. Batzill, "Surface science studies of gas sensing materials: SnO_2," *Sensors*, vol. 6, no. 10, pp. 1345–1366, 2006.

[77] D. K. Smith and W. Newkirk, "The crystal structure of baddeleyite (monoclinic ZrO_2) and its relation to the polymorphism of ZrO_2," *Acta Crystallographica*, vol. 18, no. 6, pp. 983–991, 1965.

[78] F. Haase and J. Sauer, "The surface structure of sulfated zirconia: periodic ab initio study of sulfuric acid adsorbed on ZrO_2 (101) and ZrO_2 (001)," *Journal of the American Chemical Society*, vol. 120, no. 51, pp. 13503–13512, 1998.

[79] G. Teufer, "The crystal structure of tetragonal ZrO_2," *Acta Crystallographica*, vol. 15, no. 11, p. 1187, 1962.

[80] D. K. Smith and C. F. Cline, "Verification of existence of cubic zirconia at high temperature," *Journal of the American Ceramic Society*, vol. 45, no. 5, pp. 249-250, 1962.

[81] B. Akgenc and T. Cagin, "Density functional theory of cubic zirconia and 6–15 mol% doped yttria-stabilized zirconia: structural and mechanical properties," *Turkish Journal of Physics*, vol. 42, pp. 223–231, 2018.

[82] C. Morterra, G. Cerrato, L. Ferroni, A. Negro, and L. Montanaro, "Surface characterization of tetragonal ZrO_2," *Applied Surface Science*, vol. 65-66, pp. 257–264, 1993.

[83] A. Hofmann, S. J. Clark, M. Oppel, and I. Hahndorf, "Hydrogen adsorption on the tetragonal ZrO_2(101) surface: a theoretical study of an important catalytic reactant," *Physical Chemistry Chemical Physics*, vol. 4, no. 14, pp. 3500–3508, 2002.

[84] A. Christensen and E. A. Carter, "First-principles study of the surfaces of zirconia," *Physical Review B*, vol. 58, no. 12, pp. 8050–8064, 1998.

[85] A. Eichler and G. Kresse, "First-principles calculations for the surface termination of pure and yttria-doped zirconia surfaces," *Physical Review B*, vol. 69, no. 4, article 045402, 2004.

[86] P. W. Tasker, "The stability of ionic crystal surfaces," *Journal of Physics C: Solid State Physics*, vol. 12, no. 22, pp. 4977–4984, 1979.

[87] R. M. Cornell and U. Schwertmann, *The Iron Oxides: Structure, Properties, Reactions, Occurrences and Uses*, Wiley-VCH, 2003.

[88] J. C. Russ, *Fractal Surface*, Springer Science+Business Media, New York, NY, USA, 1994.

[89] C. T. Campbell and J. Sauer, "Introduction: surface chemistry of oxides," *Chemical Reviews*, vol. 113, no. 6, pp. 3859–3862, 2012.

[90] R. A. van Santen, I. Tranca, and E. J. M. Hensen, "Theory of surface chemistry and reactivity of reducible oxides," *Catalysis Today*, vol. 244, pp. 63–84, 2015.

[91] Y.-F. Geng, P. Li, J.-Z. Li, X. M. Zhang, Q. D. Zeng, and C. Wang, "STM probing the supramolecular coordination chemistry on solid surface: structure, dynamic, and reactivity," *Coordination Chemistry Reviews*, vol. 337, pp. 145–177, 2017.

[92] H. H. Kung, Ed., "Transition metal oxides: surface chemistry and catalysis," *Studies in Surface Science and Catalysis*, vol. 45, pp. 1–286, 1989.

[93] R. A. V. Santen, "Theoretical heterogeneous catalysis," *World Scientific Lecture and Course Notes in Chemistry*, vol. 5, p. 322, 1991.

[94] D. R. Mullins, "The surface chemistry of cerium oxide," *Surface Science Reports*, vol. 70, no. 1, pp. 42–85, 2015.

[95] Z. Jovanovic, D. Bajuk-Bogdanović, S. Jovanović et al., "The role of surface chemistry in the charge storage properties of graphene oxide," *Electrochimica Acta*, vol. 258, pp. 1228–1243, 2017.

[96] J. R. H. Ross, Ed., *Heterogeneous Catalysis. Fundamentals and Applications*, Elsevier, 2012.

[97] M. M. Sychev, T. S. Minakova, Y. G. Slizhov, and O. A. Shilova, *Acid-Basic Characteristics of the Surface of Solids and Control of the Properties of Materials and Composites*, Khimizdat, St. Petersburg, 2016.

[98] M. A. Islam, D. W. Morton, B. B. Johnson, B. Mainali, and M. J. Angove, "Manganese oxides and their application to metal ion and contaminant removal from wastewater," *Journal of Water Process Engineering*, vol. 26, pp. 264–280, 2018.

[99] J. Rivera-Utrilla, I. Bautista-Toledo, M. . A. Ferro-García, and C. Moreno-Castilla, "Activated carbon surface modifications by adsorption of bacteria and their effect on aqueous lead adsorption," *Journal of Chemical Technology & Biotechnology*, vol. 76, no. 12, pp. 1209–1215, 2001.

[100] A. Piscopo, D. Robert, and J. V. Weber, "Influence of pH and chloride anion on the photocatalytic degradation of organic compounds," *Applied Catalysis B: Environmental*, vol. 35, no. 2, pp. 117–124, 2001.

[101] M. Fukuta, N. Zettsu, I. Yamashita, Y. Uraoka, and H. Watanabe, "The adsorption mechanism of titanium-binding ferritin to amphoteric oxide," *Colloids and Surfaces B: Biointerfaces*, vol. 102, pp. 435–440, 2013.

[102] S. Nagirnyak, V. Lutz, T. Dontsova, and I. Astrelin, "The effect of the synthesis conditions on morphology of tin (IV) oxide obtained by vapor transport method," *Nanophysics, Nanophotonics, Surface Studies, and Applications*, vol. 183, p. 331, 2016.

[103] S.–. C. Chang, "Oxygen chemisorption on tin oxide: correlation between electrical conductivity and EPR measurements," *Journal of Vacuum Science and Technology*, vol. 17, no. 1, pp. 366–369, 1980.

[104] J. Matos, S. Miralles-Cuevas, A. Ruíz-Delgado, I. Oller, and S. Malato, "Development of TiO_2-C photocatalysts for solar treatment of polluted water," *Carbon*, vol. 122, pp. 361–373, 2017.

[105] M. Shafaee, E. K. Goharshadi, M. Mashreghi, and M. Sadeghinia, "TiO_2 nanoparticles and TiO_2@graphene quantum dots nancomposites as effective visible/solar light photocatalysts," *Journal of Photochemistry and Photobiology A: Chemistry*, vol. 357, pp. 90–102, 2018.

[106] J. Archana, S. Harish, S. Kavirajan et al., "Ultra-fast photocatalytic and dye-sensitized solar cell performances of mesoporous TiO_2 nanospheres," *Applied Surface Science*, vol. 449, pp. 729–735, 2018.

[107] Z. Shayegan, C.-S. Lee, and F. Haghighat, "TiO_2 photocatalyst for removal of volatile organic compounds in gas phase—a review," *Chemical Engineering Journal*, vol. 334, pp. 2408–2439, 2018.

[108] R. Murugan and C. Ganesh Ram, "Energy efficient drinking water purification system using TiO_2 solar reactor with traditional methods," *Materials Today: Proceedings*, vol. 5, no. 1, pp. 415–421, 2018.

[109] S. Kathirvel, H.-S. Chen, C. Su, H. H. Wang, C. Y. Li, and W. R. Li, "Preparation of smooth surface TiO_2 photoanode for high energy conversion efficiency in dye-sensitized solar cells," *Journal of Nanomaterials*, vol. 2013, Article ID 367510, 8 pages, 2013.

[110] S. G. Kumar and K. S. R. Koteswara Rao, "Zinc oxide based photocatalysis: tailoring surface-bulk structure and related interfacial charge carrier dynamics for better environmental applications," *RSC Advances*, vol. 5, no. 5, pp. 3306–3351, 2015.

[111] S. Nahirniak, T. Dontsova, and I. Astrelin, "Directional synthesis of SnO_2-based nanostructures for use in gas sensors," *Nanochemistry, Biotechnology, Nanomaterials, and Their Applications*, vol. 214, pp. 233–245, 2018.

[112] L. X. Lovisa, V. D. Araújo, R. L. Tranquilin et al., "White photoluminescence emission from ZrO_2 co-doped with Eu^{3+}, Tb^{3+} and Tm^{3+}," *Journal of Alloys and Compounds*, vol. 674, pp. 245–251, 2016.

[113] A. Zheng, S. J. Huang, Q. Wang, H. Zhang, F. Deng, and S. B. Liu, "Progress in development and application of solid-state NMR for solid acid catalysis," *Chinese Journal of Catalysis*, vol. 34, no. 3, pp. 436–491, 2013.

[114] M. C. Muñoz, S. Gallego, J. I. Beltrán, and J. Cerdá, "Adhesion at metal-ZrO_2 interfaces," *Surface Science Reports*, vol. 61, no. 7, pp. 303–344, 2006.

[115] A. Saxena, N. Singh, D. Kumar, and P. Gupta, "Effect of ceramic reinforcement on the properties of metal matrix nanocomposites," *Materials Today: Proceedings*, vol. 4, no. 4, pp. 5561–5570, 2017.

[116] G. Soon, B. Pingguan-Murphy, K. W. Lai, and S. A. Akbar, "Review of zirconia-based bioceramic: surface modification and cellular response," *Ceramics International*, vol. 42, no. 11, pp. 12543–12555, 2016.

[117] Y. L. Bruni, L. B. Garrido, and E. F. Aglietti, "Effect of high alumina cement on permeability and structure properties of ZrO_2 composites," *Ceramics International*, vol. 38, no. 3, pp. 1755–1763, 2012.

[118] M. E. Zorn, D. T. Tompkins, W. A. Zeltner, and M. A. Anderson, "Photocatalytic oxidation of acetone vapor on TiO_2/ZrO_2 thin films," *Applied Catalysis B: Environmental*, vol. 23, no. 1, pp. 1–8, 1999.

[119] K. Hayek, R. Kramer, and Z. Paál, "Metal-support boundary sites in catalysis," *Applied Catalysis A: General*, vol. 162, no. 1–2, pp. 1–15, 1997.

[120] N. I. de Azevedo Lopes, L. de Arruda Santos, and V. T. L. Buono, "Mechanical properties of nanoceramic zirconia coatings on NiTi orthodontic wires," *Advances in Science and Technology*, vol. 97, pp. 147–152, 2016.

[121] M. O. Curi, H. C. Ferraz, J. G. M. Furtado, and A. R. Secchi, "Dispersant effects on YSZ electrolyte characteristics for solid oxide fuel cells," *Ceramics International*, vol. 41, no. 5, pp. 6141–6148, 2015.

[122] S. R. Hui, J. Roller, S. Yick et al., "A brief review of the ionic conductivity enhancement for selected oxide electrolytes," *Journal of Power Sources*, vol. 172, no. 2, pp. 493–502, 2007.

[123] P. Nadoll, T. Angerer, J. L. Mauk, D. French, and J. Walshe, "The chemistry of hydrothermal magnetite: a review," *Ore Geology Reviews*, vol. 61, pp. 1–32, 2014.

[124] O. Makarchuk, T. Dontsova, A. Perekos, A. Skoblik, and Y. Svystunov, "Magnetic mineral nanocomposite sorbents for wastewater treatment," *Journal of Nanomaterials*, vol. 2017, Article ID 8579598, 7 pages, 2017.

[125] R. A. Revia and M. Zhang, "Magnetite nanoparticles for cancer diagnosis, treatment, and treatment monitoring: recent advances," *Materials Today*, vol. 19, no. 3, pp. 157–168, 2016.

[126] J. Leitner, V. Bartůněk, D. Sedmidubský, and O. Jankovský, "Thermodynamic properties of nanostructured ZnO," *Applied Materials Today*, vol. 10, pp. 1–11, 2018.

[127] J. Zheng, J. Xiao, and J.-G. Zhang, "The roles of oxygen non-stoichiometry on the electrochemical properties of oxide-based cathode materials," *Nano Today*, vol. 11, no. 5, pp. 678–694, 2016.

[128] W.-J. Yin, B. Wen, C. Zhou, A. Selloni, and L. M. Liu, "Excess electrons in reduced rutile and anatase TiO_2," *Surface Science Reports*, vol. 73, no. 2, pp. 58–82, 2018.

[129] F. Xu, "Review of analytical studies on TiO_2 nanoparticles and particle aggregation, coagulation, flocculation, sedimentation, stabilization," *Chemosphere*, vol. 212, pp. 662–677, 2018.

[130] N. Arconada, A. Durán, S. Suárez et al., "Synthesis and photocatalytic properties of dense and porous TiO_2-anatase thin films prepared by sol-gel," *Applied Catalysis B: Environmental*, vol. 86, no. 1–2, pp. 1–7, 2009.

[131] Z. Fan and J. G. Lu, "Zinc oxide nanostructures: synthesis and properties," *Journal of Nanoscience and Nanotechnology*, vol. 5, no. 10, pp. 1561–1573, 2005.

[132] Z. L. Wang, "Zinc oxide nanostructures: growth, properties and applications," *Journal of Physics: Condensed Matter*, vol. 16, pp. 829–858, 2004.

[133] L. Renuka, K. S. Anantharaju, S. C. Sharma et al., "Hollow microspheres Mg-doped ZrO_2 nanoparticles: green assisted synthesis and applications in photocatalysis and photoluminescence," *Journal of Alloys and Compounds*, vol. 672, pp. 609–622, 2016.

[134] A. Król, P. Pomastowski, K. Rafińska, V. Railean-Plugaru, and B. Buszewski, "Zinc oxide nanoparticles: synthesis, antiseptic activity and toxicity mechanism," *Advances in Colloid and Interface Science*, vol. 249, pp. 37–52, 2017.

[135] J. Zhang and A. Yu, "Nanostructured transition metal oxides as advanced anodes for lithium-ion batteries," *Science Bulletin*, vol. 60, no. 9, pp. 823–838, 2015.

[136] S. Mallakpour and E. Khadem, "Carbon nanotube-metal oxide nanocomposites: fabrication, properties and applications," *Chemical Engineering Journal*, vol. 302, pp. 344–367, 2016.

[137] T. A. Dontsova, L. M. Kulikov, and I. M. Astrelin, "Adsorption photocataltic properties of micronic and graphene (2D) nanoparticles of molybdenum dichalcogenides," *Journal of Water Chemistry and Technology*, vol. 39, no. 3, pp. 132–137, 2017.

[138] X. Carrier, S. Royer, and E. Marceau, "Chapter 2. Synthesis of metal oxide catalysts," in *Metal Oxides in Heterogeneous Catalysis*, pp. 43–103, Elsevier, 2018.

[139] K. Naseem, Z. H. Farooqi, R. Begum, and A. Irfan, "Removal of Congo red dye from aqueous medium by its catalytic reduction using sodium borohydride in the presence of various inorganic nano-catalysts: a review," *Journal of Cleaner Production*, vol. 187, pp. 296–307, 2018.

[140] S. B. Singh and P. K. Tandon, "Catalysis: a brief review on nano-catalyst," *Journal of Energy and Chemical Engineering*, vol. 2, no. 3, pp. 106–115, 2014.

[141] M. Landmann, E. Rauls, and W. G. Schmidt, "The electronic structure and optical response of rutile, anatase and brookite TiO_2," *Journal of Physics: Condensed Matter*, vol. 24, no. 19, pp. 195503–195506, 2012.

[142] N. Rahimi, R. A. Pax, and E. M. A. Gray, "Review of functional titanium oxides. I: TiO_2 and its modifications," *Progress in Solid State Chemistry*, vol. 44, no. 3, pp. 86–105, 2016.

[143] H. Zangeneh, A. A. L. Zinatizadeh, M. Habibi, M. Akia, and M. Hasnain Isa, "Photocatalytic oxidation of organic dyes

and pollutants in wastewater using different modified titanium dioxides: a comparative review," *Journal of Industrial and Engineering Chemistry*, vol. 26, pp. 1–36, 2015.

[144] M. R. D. Khaki, M. S. Shafeeyan, A. A. A. Raman, and W. M. A. W. Daud, "Application of doped photocatalysts for organic pollutant degradation—a review," *Journal of Environmental Management*, vol. 198, Part 2, pp. 78–94, 2017.

[145] J. Wen, X. Li, W. Liu, Y. Fang, J. Xie, and Y. Xu, "Photocatalysis fundamentals and surface modification of TiO_2 nanomaterials," *Chinese Journal of Catalysis*, vol. 36, no. 12, pp. 2049–2070, 2015.

[146] Y. Liu, L. Tian, X. Tan, X. Li, and X. Chen, "Synthesis, properties, and applications of black titanium dioxide nanomaterials," *Science Bulletin*, vol. 62, no. 6, pp. 431–441, 2017.

[147] K. Fischer, A. Gawel, D. Rosen et al., "Low-temperature synthesis of anatase/rutile/brookite TiO_2 nanoparticles on a polymer membrane for photocatalysis," *Catalysts*, vol. 7, no. 7, p. 209, 2017.

[148] Y. Liao and W. Que, "Preparation and photocatalytic activity of TiO_2 nanotube powders derived by a rapid anodization process," *Journal of Alloys and Compounds*, vol. 505, no. 1, pp. 243–248, 2010.

[149] J. Yu and B. Wang, "Effect of calcination temperature on morphology and photoelectrochemical properties of anodized titanium dioxide nanotube arrays," *Applied Catalysis B: Environmental*, vol. 94, no. 3-4, pp. 295–302, 2010.

[150] S.-J. Kim, E. G. Lee, S. D. Park et al., "Photocatalytic effects of rutile phase TiO_2 ultrafine powder with high specific surface area obtained by a homogeneous precipitation process at low temperatures," *Journal of Sol-Gel Science and Technology*, vol. 22, no. 1/2, pp. 63–74, 2001.

[151] M. I. H. Chowdhury, M. S. Hossain, M. A. S. Azad et al., "Photocatalytic degradation of methyl orange under UV using ZnO as catalyst," *International Journal of Scientific & Engineering Research*, vol. 9, no. 6, pp. 1646–1649, 2018.

[152] N. A. Yusoff, S.-A. Ong, L.-N. Ho, Y. S. Wong, and W. F. Khalik, "Degradation of phenol through solar-photocatalytic treatment by zinc oxide in aqueous solution," *Desalination and Water Treatment*, vol. 54, pp. 1–8, 2014.

[153] A. Akyol and M. Bayramoğlu, "Photocatalytic degradation of Remazol Red F3B using ZnO catalyst," *Journal of Hazardous Materials*, vol. 124, no. 1–3, pp. 241–246, 2005.

[154] L. Zhu and W. Zeng, "Room-temperature gas sensing of ZnO-based gas sensor: a review," *Sensors and Actuators A: Physical*, vol. 267, pp. 242–261, 2017.

[155] P. Struk, T. Pustelny, K. Gołaszewska, M. A. Borysiewicz, and A. Piotrowska, "Gas sensors based on ZnO structures," *Acta Physica Polonica A*, vol. 124, no. 3, pp. 567–569, 2013.

[156] L. Li, T. Zhai, Y. Bando, and D. Golberg, "Recent progress of one-dimensional ZnO nanostructured solar cells," *Nano Energy*, vol. 1, no. 1, pp. 91–106, 2012.

[157] P. Yang, H. Yan, S. Mao et al., "Controlled growth of ZnO nanowires and their optical properties," *Advanced Functional Materials*, vol. 12, no. 5, pp. 323–331, 2002.

[158] C. M. Lieber and Z. L. Wang, "Functional nanowires," *MRS Bulletin*, vol. 32, no. 2, pp. 99–108, 2007.

[159] X. Fang, Y. Bando, U. K. Gautam, C. Ye, and D. Golberg, "Inorganic semiconductor nanostructures and their field-emission applications," *Journal of Materials Chemistry*, vol. 18, no. 5, pp. 509–522, 2008.

[160] Y. Wang, M. Wu, Z. Jiao, and J. Y. Lee, "One-dimensional SnO_2 nanostructures: facile morphology tuning and lithium storage properties," *Nanotechnology*, vol. 20, no. 34, article 345704, 2009.

[161] N. Ramgir, N. Datta, M. Kaur et al., "Metal oxide nanowires for chemiresistive gas sensors: issues, challenges and prospects," *Colloids and Surfaces A: Physicochemical and Engineering Aspects*, vol. 439, pp. 101–116, 2013.

[162] S. Choopun, N. Hongsith, and E. Wongrat, "Chapter 1. Metal-oxide nanowires for gas sensors," in *Nanowires*, pp. 3–24, IntechOpen Limited, London, 2012.

[163] A. Galadima and O. Muraza, "A review on glycerol valorization to acrolein over solid acid catalysts," *Journal of the Taiwan Institute of Chemical Engineers*, vol. 67, pp. 29–44, 2016.

[164] A. Chieregato, J. M. López Nieto, and F. Cavani, "Mixed-oxide catalysts with vanadium as the key element for gas-phase reactions," *Coordination Chemistry Reviews*, vol. 301-302, pp. 3–23, 2015.

[165] A. Azzouz, S. K. Kailasa, S. S. Lee et al., "Review of nanomaterials as sorbents in solid-phase extraction for environmental samples," *TrAC Trends in Analytical Chemistry*, vol. 108, pp. 347–369, 2018.

[166] R. Liu, L. Chi, X. Wang, Y. Sui, Y. Wang, and H. Arandiyan, "Review of metal (hydr)oxide and other adsorptive materials for phosphate removal from water," *Journal of Environmental Chemical Engineering*, vol. 6, no. 4, pp. 5269–5286, 2018.

[167] N. Yamazoe, "Toward innovations of gas sensor technology," *Sensors and Actuators B*, vol. 108, no. 1-2, pp. 2–14, 2005.

[168] L. B. Tahar, M. H. Oueslati, and M. J. A. Abualreish, "Synthesis of magnetite derivatives nanoparticles and their application for the removal of chromium (VI) from aqueous solutions," *Journal of Colloid and Interface Science*, vol. 512, pp. 115–126, 2018.

[169] R. D. Ambashta and M. Sillanpää, "Water purification using magnetic assistance: a review," *Journal of Hazardous Materials*, vol. 180, no. 1–3, pp. 38–49, 2010.

[170] A. R. Mahdavian and M. A.-S. Mirrahimi, "Efficient separation of heavy metal cations by anchoring polyacrylic acid on superparamagnetic magnetite nanoparticles through surface modification," *Chemical Engineering Journal*, vol. 159, no. 1–3, pp. 264–271, 2010.

[171] P. Xu, G. M. Zeng, D. L. Huang et al., "Use of iron oxide nanomaterials in wastewater treatment: a review," *Science of the Total Environment*, vol. 424, pp. 1–10, 2012.

[172] X. Hu, G. Li, and J. C. Yu, "Design, fabrication, and modification of nanostructured semiconductor materials for environmental and energy applications," *Langmuir*, vol. 26, no. 5, pp. 3031–3039, 2010.

[173] F.-L. Fan, Z. Qin, J. Bai et al., "Rapid removal of uranium from aqueous solutions using magnetic Fe_3O_4@SiO_2 composite particles," *Journal of Environmental Radioactivity*, vol. 106, pp. 40–46, 2012.

[174] D. Jing and D. Song, "Optical properties of nanofluids considering particle size distribution: experimental and theoretical investigations," *Renewable and Sustainable Energy Reviews*, vol. 78, pp. 452–465, 2017.

[175] Y. Xianyu, Q. Wang, and Y. Chen, "Magnetic particles-enabled biosensors for point-of-care testing," *TrAC Trends in Analytical Chemistry*, vol. 106, pp. 213–224, 2018.

[176] D. Lisjak and A. Mertelj, "Anisotropic magnetic nanoparticles: a review of their properties, syntheses and potential

applications," *Progress in Materials Science*, vol. 95, pp. 286–328, 2018.

[177] J. M. Munyalo and X. Zhang, "Particle size effect on thermophysical properties of nanofluid and nanofluid based phase change materials: a review," *Journal of Molecular Liquids*, vol. 265, pp. 77–87, 2018.

[178] P. A. Maurice and M. F. Hochella, "Chapter 5. Nanoscale particles and processes: a new dimension in soil science," *Advances in Agronomy*, vol. 100, pp. 123–153, 2008.

[179] M. Dragoman and D. Dragoman, "Plasmonics: applications to nanoscale terahertz and optical devices," *Progress in Quantum Electronics*, vol. 32, no. 1, pp. 1–41, 2008.

[180] S. Hashimoto, D. Werner, and T. Uwada, "Studies on the interaction of pulsed lasers with plasmonic gold nanoparticles toward light manipulation, heat management, and nanofabrication," *Journal of Photochemistry and Photobiology C: Photochemistry Reviews*, vol. 13, no. 1, pp. 28–54, 2012.

[181] Z. Li, H. Jiang, C. Xu, and L. Gu, "A review: using nanoparticles to enhance absorption and bioavailability of phenolic phytochemicals," *Food Hydrocolloids*, vol. 43, pp. 153–164, 2015.

[182] D. Kandi, S. Martha, and K. M. Parida, "Quantum dots as enhancer in photocatalytic hydrogen evolution: a review," *International Journal of Hydrogen Energy*, vol. 42, no. 15, pp. 9467–9481, 2017.

[183] L. Moro, M. Turemis, B. Marini, R. Ippodrino, and M. T. Giardi, "Better together: strategies based on magnetic particles and quantum dots for improved biosensing," *Biotechnology Advances*, vol. 35, no. 1, pp. 51–63, 2017.

[184] A. Dan, H. C. Barshilia, K. Chattopadhyay, and B. Basu, "Solar energy absorption mediated by surface plasma polaritons in spectrally selective dielectric-metal-dielectric coatings: a critical review," *Renewable and Sustainable Energy Reviews*, vol. 79, pp. 1050–1077, 2017.

[185] R. Tucceri, "A review about the surface resistance technique in electrochemistry," *Surface Science Reports*, vol. 56, no. 3–4, pp. 85–157, 2004.

[186] F. Pan, C. Song, X. J. Liu, Y. C. Yang, and F. Zeng, "Ferromagnetism and possible application in spintronics of transition-metal-doped ZnO films," *Materials Science and Engineering: R: Reports*, vol. 62, no. 1, pp. 1–35, 2008.

[187] S. J. Lee, S. Souma, G. Ihm, and K. J. Chang, "Magnetic quantum dots and magnetic edge states," *Physics Reports*, vol. 394, no. 1, pp. 1–40, 2004.

[188] J. Pan, H. Shen, and S. Mathur, "One-dimensional SnO_2 nanostructures: synthesis and applications," *Journal of Nanotechnology*, vol. 2012, Article ID 917320, 12 pages, 2012.

[189] T. Zhai, X. Fang, M. Liao et al., "A comprehensive review of one-dimensional metal-oxide nanostructure photodetectors," *Sensors*, vol. 9, no. 8, pp. 6504–6529, 2009.

[190] M. M. Arafat, B. Dinan, S. A. Akbar, and A. S. M. A. Haseeb, "Gas sensors based on one dimensional nanostructured metal-oxides: a review," *Sensors*, vol. 12, no. 6, pp. 7207–7258, 2012.

[191] T. A. Dontsova, S. V. Nagirnyak, V. V. Zhorov, and Y. V. Yasiievych, "SnO_2 nanostructures: effect of processing parameters on their structural and functional properties," *Nanoscale Research Letters*, vol. 12, no. 1, pp. 332–337, 2017.

[192] C. Guillén and J. Herrero, "TCO/metal/TCO structures for energy and flexible electronics," *Thin Solid Films*, vol. 520, no. 1, pp. 1–17, 2011.

[193] K. Ellmer, R. Mientus, and S. Seeger, "Metallic oxides (ITO, ZnO, SnO_2, TiO_2)," in *Transparent Conductive Materials: Materials, Synthesis, Characterization, Applications*, pp. 31–80, Wiley-VCH Verlag GmbH & Co. KGaA, 2018.

[194] G. Yang, Z. Yan, and T. Xiao, "Preparation and characterization of SnO_2/ZnO/TiO_2 composite semiconductor with enhanced photocatalytic activity," *Applied Surface Science*, vol. 258, no. 22, pp. 8704–8712, 2012.

[195] K. Rajeshwar, M. E. Osugi, W. Chanmanee et al., "Heterogeneous photocatalytic treatment of organic dyes in air and aqueous media," *Journal of Photochemistry and Photobiology C: Photochemistry Reviews*, vol. 9, no. 4, pp. 171–192, 2008.

[196] A. McEvoy, L. Castañer, and T. Markvart, Eds., *Solar Cells: Materials, Manufacture and Operation*, 2nd edition2nd edition, , 2013.

[197] M. E. Osugi, M. V. B. Zanoni, C. R. Chenthamarakshan et al., "Toxicity assessment and degradation of disperse azo dyes by photoelectrocatalytic oxidation on Ti/TiO_2 nanotubular array electrodes," *Journal of Advanced Oxidation Technologies*, vol. 11, no. 3, pp. 425–434, 2008.

[198] T. Sekino, "Synthesis and applications of titanium oxide nanotubes," *Inorganic and Metallic Nanotubular Materials*, vol. 117, pp. 17–32, 2010.

[199] S. Munnix and M. Schmeits, "Surface electronic structure of SnO_2(110)," *Solid State Communications*, vol. 43, no. 11, pp. 867–871, 1982.

[200] T. A. Miller, S. D. Bakrania, C. Perez, and M. S. Wooldridge, "Nanosturctured tin dioxide materials for gas sensor applications," *Functional Nanomaterials*, vol. 30, pp. 1–24, 2006.

[201] D. Barreca, D. Bekermann, E. Comini et al., "1D ZnO nanoassemblies by plasma-CVD as chemical sensors for flammable and toxic gases," *Sensors and Actuators B: Chemical*, vol. 149, no. 1, pp. 1–7, 2010.

[202] A. Iannaci, B. Mecheri, A. D'Epifanio, and S. Licoccia, "Sulfated zirconium oxide as electrode and electrolyte additive for direct methanol fuel cell applications," *International Journal of Hydrogen Energy*, vol. 39, no. 21, pp. 11241–11249, 2014.

[203] Y. Hirata, S. Daio, A. Kai et al., "Performance of yttria-stabilized zirconia fuel cell using H_2-CO_2 gas system and CO-O_2 gas system," *Ceramics International*, vol. 42, no. 16, pp. 18373–18379, 2016.

[204] D. A. Agarkov, M. A. Borik, V. T. Bublik et al., "Structure and transport properties of melt grown Sc_2O_3 and CeO_2 doped ZrO_2 crystals," *Solid State Ionics*, vol. 322, pp. 24–29, 2018.

[205] H. Kwak and S. Chaudhuri, "Role of vacancy and metal doping on combustive oxidation of Zr/ZrO_2 core-shell particles," *Surface Science*, vol. 604, no. 23–24, pp. 2116–2128, 2010.

[206] A. S. Teja and P.-Y. Koh, "Synthesis, properties, and applications of magnetic iron oxide nanoparticles," *Progress in Crystal Growth and Characterization of Materials*, vol. 55, no. 1–2, pp. 22–45, 2009.

[207] S. P. Gubin, Y. A. Koksharov, G. B. Khomutov, and G. Y. Yurkov, "Magnetic nanoparticles: production methods, structure and properties," *Successes Chemistry*, vol. 74, no. 6, pp. 539–574, 2005.

[208] G. E. Zilberman, *Electricity and Magnetism*, Science, Moscow, 1970.

[209] A. Moezzi, A. M. McDonagh, and M. B. Cortie, "Zinc oxide particles: synthesis, properties and applications," *Chemical Engineering Journal*, vol. 185-186, pp. 1–22, 2012.

[210] S. Das and V. Jayaraman, "SnO_2: a comprehensive review on structures and gas sensors," *Progress in Materials Science*, vol. 66, pp. 112–255, 2014.

[211] S. Park, S. Lim, and H. Choi, "Chemical vapor deposition of iron and iron oxide thin films from Fe(II) dihydride complexes," *Chemistry of Materials*, vol. 18, no. 22, pp. 5150–5152, 2006.

[212] M. J. Lawrence, A. Kolodziej, and P. Rodriguez, "Controllable synthesis of nanostructured metal oxide and oxyhydroxide materials via electrochemical methods," *Current Opinion in Electrochemistry*, vol. 10, pp. 7–15, 2018.

[213] I. N. Ivanenko, T. A. Dontsova, I. M. Astrelin, and V. V. Trots, "Low-temperature synthesis, structure-sorption characterisics and photocatalytic activity of TiO_2 nanostructures," *Journal of Water Chemistry and Technology*, vol. 38, no. 1, pp. 14–20, 2016.

[214] G. Chatel, "Sonochemistry in nanocatalysis: the use of ultrasound from the catalyst synthesis to the catalytic reaction," *Current Opinion in Green and Sustainable Chemistry*, vol. 15, pp. 1–6, 2019.

[215] C. Y. Teh, T. Y. Wu, and J. C. Juan, "An application of ultrasound technology in synthesis of titania-based photocatalyst for degrading pollutant," *Chemical Engineering Journal*, vol. 317, pp. 586–612, 2017.

[216] S. Vallejos, F. di Maggio, T. Shujah, and C. Blackman, "Chemical vapour deposition of gas sensitive metal oxides," *Chemosensors*, vol. 4, no. 1, pp. 4–18, 2016.

[217] D. Zappa, V. Galstyan, N. Kaur, H. M. M. Munasinghe Arachchige, O. Sisman, and E. Comini, "Metal oxide-based heterostructures for gas sensors: a review," *Analytica Chimica Acta*, vol. 1039, pp. 1–23, 2018.

[218] Y. Luo, C. Zhang, B. Zheng, X. Geng, and M. Debliquy, "Hydrogen sensors based on noble metal doped metal-oxide semiconductor: a review," *International Journal of Hydrogen Energy*, vol. 42, no. 31, pp. 20386–20397, 2017.

[219] F. C. Vásquez, F. Paraguay-Delgado, J. E. Morales-Mendoza et al., "Shape and size controlled growth of SnO_2 nanoparticles by efficient approach," *Superlattices and Microstructures*, vol. 90, pp. 274–287, 2016.

[220] W. Wei, Z. Wang, Z. Liu et al., "Metal oxide hollow nanostructures: fabrication and Li storage performance," *Journal of Power Sources*, vol. 238, pp. 376–387, 2013.

[221] L. Qiao and M. T. Swihart, "Solution-phase synthesis of transition metal oxide nanocrystals: morphologies, formulae, and mechanisms," *Advances in Colloid and Interface Science*, vol. 244, pp. 199–266, 2017.

[222] G. L. J. P. da Silva, M. L. C. P. da Silva, and T. Caetano, "Preparation and characterization of hydrous zirconium oxide formed by homogeneous precipitation," *Materials Research*, vol. 5, no. 2, pp. 149–153, 2002.

[223] Q. Yang, Z. Lu, J. Liu et al., "Metal oxide and hydroxide nanoarrays: hydrothermal synthesis and applications as supercapacitors and nanocatalysts," *Progress in Natural Science: Materials International*, vol. 23, no. 4, pp. 351–366, 2013.

[224] H. Ou and S. Lo, "Review of titania nanotubes synthesized via the hydrothermal treatment: fabrication, modification, and application," *Separation and Purification Technology*, vol. 58, no. 1, pp. 179–191, 2007.

[225] D. C. Manfroi, A. dos Anjos, A. A. Cavalheiro, L. A. Perazolli, J. A. Varela, and M. A. Zaghete, "Titanate nanotubes produced from microwave-assisted hydrothermal synthesis: photocatalytic and structural properties," *Ceramics International*, vol. 40, no. 9, pp. 14483–14491, 2014.

[226] E. Arpaç, F. Sayılkan, M. Asiltürk, P. Tatar, N. Kiraz, and H. Sayılkan, "Photocatalytic performance of Sn-doped and undoped TiO_2 nanostructured thin films under UV and vis-lights," *Journal of Hazardous Materials*, vol. 140, no. 1–2, pp. 69–74, 2007.

[227] M. Á. L. Zavala, S. A. L. Morales, and M. Ávila-Santos, "Synthesis of stable TiO_2 nanotubes: effect of hydrothermal treatment, acid washing and annealing temperature," *Heliyon*, vol. 3, no. 11, article e00456, 2017.

[228] A. Solmaz, S. Balci, and T. Dogu, "Synthesis and characterization of V, Mo and Nb incorporated micro–mesoporous MCM-41 materials," *Materials Chemistry and Physics*, vol. 125, no. 1–2, pp. 148–155, 2011.

[229] B. K. Mutuma, G. N. Shao, W. D. Kim, and H. T. Kim, "Sol-gel synthesis of mesoporous anatase-brookite and anatase-brookite-rutile TiO_2 nanoparticles and their photocatalytic properties," *Journal of Colloid and Interface Science*, vol. 442, pp. 1–7, 2015.

[230] Z. Li, Z. J. Yao, A. A. Haidry et al., "Resistive-type hydrogen gas sensor based on TiO_2: a review," *International Journal of Hydrogen Energy*, vol. 43, no. 45, pp. 21114–21132, 2018.

[231] O. Carp, C. L. Huisman, and A. Reller, "Photoinduced reactivity of titanium dioxide," *Progress in Solid State Chemistry*, vol. 32, no. 1–2, pp. 33–177, 2004.

[232] A. Kutuzova and T. Dontsova, "Synthesis, characterization and properties of titanium dioxide obtained by hydrolytic method," in *2017 IEEE 7th International Conference Nanomaterials: Application & Properties (NAP)*, pp. 01NNPT02-1–01NNPT02-5, Odessa, Ukraine, 2017.

[233] T. Dontsova, I. Ivanenko, and I. Astrelin, "Synthesis and characterization of titanium (IV) oxide from various precursors," *Nanoplasmonics, Nano-Optics, Nanocomposites, and Surface Studies*, vol. 167, pp. 275–293, 2015.

[234] J. G. Lu, P. Chang, and Z. Fan, "Quasi-one-dimensional metal oxide materials—synthesis, properties and applications," *Materials Science and Engineering: R: Reports*, vol. 52, no. 1–3, pp. 49–91, 2006.

[235] B. B. Wang, K. Zhu, J. Feng et al., "Low-pressure thermal chemical vapour deposition of molybdenum oxide nanorods," *Journal of Alloys and Compounds*, vol. 661, pp. 66–71, 2016.

[236] H. Coskun, A. Aljabour, L. Uiberlacker et al., "Chemical vapor deposition-based synthesis of conductive polydopamine thin-films," *Thin Solid Films*, vol. 645, pp. 320–325, 2018.

[237] S. V. Nagirnyak, V. A. Lutz, T. A. Dontsova, and I. M. Astrelin, "Synthesis and characterization of tin (IV) oxide obtained by chemical vapor deposition method," *Nanoscale Research Letters*, vol. 11, no. 1, pp. 343–347, 2016.

[238] E. Comini, "Metal oxide nano-crystals for gas sensing," *Analytica Chimica Acta*, vol. 568, no. 1–2, pp. 28–40, 2006.

[239] M. K. Baek, S. J. Park, and D. J. Choi, "Synthesis of zirconia (ZrO_2) nanowires via chemical vapor deposition," *Journal of Crystal Growth*, vol. 459, pp. 198–202, 2017.

[240] K. Assim, J. Jeschke, A. Jakob et al., "Manganese half-sandwich complexes as metal-organic chemical vapor deposition precursors for manganese-based thin films," *Thin Solid Films*, vol. 619, pp. 265–272, 2016.

[241] C. J. Brinker and D. R. Dunphy, "Morphological control of surfactant-templated metal oxide films," *Current Opinion in Colloid & Interface Science*, vol. 11, no. 2–3, pp. 126–132, 2006.

[242] L. Zhang, W. Yu, C. Han et al., "Large scaled synthesis of heterostructured electrospun TiO_2/SnO_2 nanofibers with an enhanced photocatalytic activity," *Journal of the Electrochemical Society*, vol. 164, no. 9, pp. H651–H656, 2017.

[243] J. Gong, H. Qiao, S. Sigdel et al., "Characteristics of SnO_2 nanofiber/TiO_2 nanoparticle composite for dye-sensitized solar cells," *AIP Advances*, vol. 5, no. 6, article 067134, 2015.

[244] G. Elango and S. M. Roopan, "Efficacy of SnO_2 nanoparticles toward photocatalytic degradation of methylene blue dye," *Journal of Photochemistry and Photobiology B: Biology*, vol. 155, pp. 34–38, 2016.

[245] M. V. Arularasu, J. Devakumar, and T. V. Rajendran, "An innovative approach for green synthesis of iron oxide nanoparticles: characterization and its photocatalytic activity," *Polyhedron*, vol. 156, pp. 279–290, 2018.

[246] A. Marzec, Z. Pędzich, and W. Maziarz, "Preparation of nanocrystalline composite TiO_2-SnO_2 powders using sol-gel method combined with hydrothermal treatment," *Processing and Application of Ceramics*, vol. 10, no. 4, pp. 249–256, 2016.

[247] K. H. Lee, H. J. Jung, J. H. Lee et al., "Facile solid-state synthesis of oxidation-resistant metal nanoparticles at ambient conditions," *Solid State Sciences*, vol. 79, pp. 38–47, 2018.

[248] Y. Fedenko, T. Dontsova, and I. Astrelin, "Physico-chemical and sorptive properties of nanocomposites based on zirconium oxide," *Chemistry & Chemical Technology*, vol. 8, no. 1, pp. 51–55, 2014.

[249] O. V. Makarchuk, T. A. Dontsova, and A. E. Perekos, "Chapter 54. Magnetic nanocomposite sorbents on mineral base," *Nanophysics, Nanomaterials, Interface Studies, and Applications*, vol. 195, pp. 705–719, 2017.

[250] X. Qu, P. J. J. Alvarez, and Q. Li, "Applications of nanotechnology in water and wastewater treatment," *Water Research*, vol. 47, no. 12, pp. 3931–3946, 2013.

[251] D. Sethi and R. Sakthivel, "ZnO/TiO_2 composites for photocatalytic inactivation of *Escherichia coli*," *Journal of Photochemistry and Photobiology B*, vol. 168, pp. 117–123, 2017.

[252] L. Chen, C. H. Zhou, S. Fiore et al., "Functional magnetic nanoparticle/clay mineral nanocomposites: preparation, magnetism and versatile applications," *Applied Clay Science*, vol. 127-128, pp. 143–163, 2016.

[253] O. Makarchuk, T. Dontsova, and G. Krymets, "Magnetic mineral nanocomposite sorbents for removal of surfactants," in *2017 IEEE 7th International Conference Nanomaterials: Application & Properties (NAP)*, pp. 02MFPM02-1–02MFPM02-6, Odessa, Ukraine, 2017.

[254] O. V. Makarchuk, T. A. Dontsova, and I. M. Astrelin, "Magnetic nanocomposites as efficient sorption materials for removing dyes from aqueous solutions," *Nanoscale Research Letters*, vol. 11, no. 1, pp. 161–167, 2016.

[255] J. Xu, X. Wang, F. Pan et al., "Synthesis of the mesoporous carbon-nano-zero-valent iron composite and activation of sulfite for removal of organic pollutants," *Chemical Engineering Journal*, vol. 353, pp. 542–549, 2018.

[256] T. Wang, L. Liang, R. Wang, Y. Jiang, K. Lin, and J. Sun, "Magnetic mesoporous carbon for efficient removal of organic pollutants," *Adsorption*, vol. 18, no. 5–6, pp. 439–444, 2012.

[257] L. Feng, M. Cao, X. Ma, Y. Zhu, and C. Hu, "Superparamagnetic high-surface-area Fe_3O_4 nanoparticles as adsorbents for arsenic removal," *Journal of Hazardous Materials*, vol. 217-218, pp. 439–446, 2012.

[258] M. Kokate, K. Garadkar, and A. Gole, "One pot synthesis of magnetite-silica nanocomposites: applications as tags, entrapment matrix and in water purification," *Journal of Materials Chemistry A*, vol. 1, no. 6, pp. 2022–2029, 2013.

[259] S. Malik, "Nanotubes from Atlantis: magnetite in pumice as a catalyst for the growth of carbon nanotubes," *Polyhedron*, vol. 152, pp. 90–93, 2018.

[260] M. F. Horst, V. Lassalle, and M. L. Ferreira, "Nanosized magnetite in low cost materials for remediation of water polluted with toxic metals, azo- and antraquinonic dyes," *Frontiers of Environmental Science & Engineering*, vol. 9, no. 5, pp. 746–769, 2015.

[261] T. A. Dontsova, E. I. Yanushevskaya, S. V. Nahirniak et al., "Directional control of the structural adsorption properties of clays by magnetite modification," *Journal of Nanomaterials*, vol. 2018, Article ID 6573016, 9 pages, 2018.

[262] E. A. Deliyanni, E. N. Peleka, and K. A. Matis, "Modeling the sorption of metal ions from aqueous solution by iron-based adsorbents," *Journal of Hazardous Materials*, vol. 172, no. 2-3, pp. 550–558, 2009.

[263] M. N. Chong, B. Jin, C. W. K. Chow, and C. Saint, "Recent developments in photocatalytic water treatment technology: a review," *Water Research*, vol. 44, no. 10, pp. 2997–3027, 2010.

[264] M. Muruganandham, R. P. S. Suri, S. Jafari et al., "Recent developments in homogeneous advanced oxidation processes for water and wastewater treatment," *International Journal of Photoenergy*, vol. 2014, Article ID 821674, 21 pages, 2014.

[265] D. B. Miklos, C. Remy, M. Jekel, K. G. Linden, J. E. Drewes, and U. Hübner, "Evaluation of advanced oxidation processes for water and wastewater treatment—a critical review," *Water Research*, vol. 139, pp. 118–131, 2018.

[266] H. Zazou, H. Afanga, S. Akhouairi et al., "Treatment of textile industry wastewater by electrocoagulation coupled with electrochemical advanced oxidation process," *Journal of Water Process Engineering*, vol. 28, pp. 214–221, 2019.

[267] C. Descorme, "Catalytic wastewater treatment: oxidation and reduction processes. Recent studies on chlorophenols?," *Catalysis Today*, vol. 297, pp. 324–334, 2017.

[268] D. Kanakaraju, B. D. Glass, and M. Oelgemöller, "Advanced oxidation process-mediated removal of pharmaceuticals from water: a review," *Journal of Environmental Management*, vol. 219, pp. 189–207, 2018.

[269] S. Jiménez, M. Andreozzi, M. M. Micó, M. G. Álvarez, and S. Contreras, "Produced water treatment by advanced oxidation processes," *Science of the Total Environment*, vol. 666, pp. 12–21, 2019.

[270] J. Khatri, P. V. Nidheesh, T. S. Anantha Singh, and M. Suresh Kumar, "Advanced oxidation processes based on zero-valent aluminium for treating textile wastewater," *Chemical Engineering Journal*, vol. 348, pp. 67–73, 2018.

[271] E. Güneş, E. Demir, Y. Güneş, and A. Hanedar, "Characterization and treatment alternatives of industrial container and drum cleaning wastewater: comparison of Fenton-like

process and combined coagulation/oxidation processes," *Separation and Purification Technology*, vol. 209, pp. 426–433, 2019.

[272] L. G. M. Silva, F. C. Moreira, A. A. U. Souza, S. M. A. G. U. Souza, R. A. R. Boaventura, and V. J. P. Vilar, "Chemical and electrochemical advanced oxidation processes as a polishing step for textile wastewater treatment: a study regarding the discharge into the environment and the reuse in the textile industry," *Journal of Cleaner Production*, vol. 198, pp. 430–442, 2018.

[273] A. Sharma, J. Ahmad, and S. J. S. Flora, "Application of advanced oxidation processes and toxicity assessment of transformation products," *Environmental Research*, vol. 167, pp. 223–233, 2018.

[274] C. W. Lai, J. C. Juan, W. B. Ko, and S. Bee Abd Hamid, "An overview: recent development of titanium oxide nanotubes as photocatalyst for dye degradation," *International Journal of Photoenergy*, vol. 2014, Article ID 524135, 14 pages, 2014.

[275] M. A. Kanjwal, N. A. M. Barakat, F. A. Sheikh, M. S. Khil, and H. Y. Kim, "Functionalization of electrospun titanium oxide nanofibers with silver nanoparticles: strongly effective photocatalyst," *International Journal of Applied Ceramic Technology*, vol. 7, pp. E54–E63, 2010.

[276] T. Pradeep and Anshup, "Noble metal nanoparticles for water purification: a critical review," *Thin Solid Films*, vol. 517, no. 24, pp. 6441–6478, 2009.

[277] F. Huang, A. Yan, and H. Zhao, "Influences of doping on photocatalytic properties of TiO_2 photocatalyst," in *Semiconductor Photocatalysis, Materials, Mechanisms and Applications*, pp. 31–80, IntechOpen, 2016.

[278] H. Park, Y. Park, W. Kim, and W. Choi, "Surface modification of TiO_2 photocatalyst for environmental applications," *Journal of Photochemistry and Photobiology C: Photochemistry Reviews*, vol. 15, pp. 1–20, 2013.

[279] M. Anpo, S. Kishiguchi, Y. Ichihashi et al., "The design and development of second-generation titanium oxide photocatalysts able to operate under visible light irradiation by applying a metal ion-implantation method," *Research on Chemical Intermediates*, vol. 27, no. 4-5, pp. 459–467, 2001.

[280] S. Ghosh and A. P. Das, "Modified titanium oxide (TiO_2) nanocomposites and its array of applications: a review," *Toxicological & Environmental Chemistry*, vol. 97, no. 5, pp. 491–514, 2015.

[281] M. Huang, J. Yu, B. Li et al., "Intergrowth and coexistence effects of TiO_2-SnO_2 nanocomposite with excellent photocatalytic activity," *Journal of Alloys and Compounds*, vol. 629, pp. 55–61, 2015.

[282] K. Majrik, E. Tálas, Z. Pászti et al., "Enhanced activity of sol-gel prepared SnO_x-TiO_2 in photocatalytic methanol reforming," *Applied Catalysis A: General*, vol. 466, pp. 169–178, 2013.

[283] I. J. Ani, U. G. Akpan, M. A. Olutoye, and B. H. Hameed, "Photocatalytic degradation of pollutants in petroleum refinery wastewater by TiO_2- and ZnO-based photocatalysts: recent development," *Journal of Cleaner Production*, vol. 205, pp. 930–954, 2018.

[284] M. Pirhashemi, A. Habibi-Yangjeh, and S. Rahim Pouran, "Review on the criteria anticipated for the fabrication of highly efficient ZnO-based visible-light-driven photocatalysts," *Journal of Industrial and Engineering Chemistry*, vol. 62, pp. 1–25, 2018.

[285] X. Chen, Z. Wu, D. Liu, and Z. Gao, "Preparation of ZnO photocatalyst for the efficient and rapid photocatalytic degradation of azo dyes," *Nanoscale Research Letters*, vol. 12, no. 1, pp. 143–148, 2017.

[286] N. Kumaresan, K. Ramamurthi, R. R. Babu, K. Sethuraman, and S. M. Babu, "Hydrothermally grown ZnO nanoparticles for effective photocatalytic activity," *Applied Surface Science*, vol. 418, pp. 138–146, 2017.

[287] K. Nakata and A. Fujishima, "TiO_2 photocatalysis: design and applications," *Journal of Photochemistry and Photobiology C: Photochemistry Reviews*, vol. 13, no. 3, pp. 169–189, 2012.

[288] S.-Y. Lee and S.-J. Park, "TiO_2 photocatalyst for water treatment applications," *Journal of Industrial and Engineering Chemistry*, vol. 19, no. 6, pp. 1761–1769, 2013.

[289] R. Lamba, A. Umar, S. K. Mehta, and S. Kumar Kansal, "Well-crystalline porous ZnO-SnO_2 nanosheets: an effective visible-light driven photocatalyst and highly sensitive smart sensor material," *Talanta*, vol. 131, pp. 490–498, 2015.

[290] S. Chaudhary, A. Umar, K. Bhasin, and S. Baskoutas, "Chemical sensing applications of ZnO nanomaterials," *Materials*, vol. 11, no. 2, p. 287, 2018.

[291] R. Kumar, O. Al-Dossary, G. Kumar, and A. Umar, "Zinc oxide nanostructures for NO_2 gas–sensor applications: a review," *Nano-Micro Letters*, vol. 7, no. 2, pp. 97–120, 2015.

[292] S. V. Nagirnyak and T. A. Dontsova, "Gas sensor device creation," in *Proceedings of the 2017 IEEE 7th International Conference on Nanomaterials: Applications and Properties*, pp. 01NNPT13-1–01NNPT13-4, Odessa, Ukraine, 2017.

[293] G. Velmathi, S. Mohan, and R. Henry, "Analysis and review of tin oxide-based chemoresistive gas sensor," *IETE Technical Review*, vol. 33, no. 3, pp. 323–331, 2015.

[294] F. A. Akgul, C. Gumus, A. O. Er et al., "Structural and electronic properties of SnO_2," *Journal of Alloys and Compounds*, vol. 579, pp. 50–56, 2013.

[295] D.-W. Cho, B.-H. Jeon, Y. Jeong et al., "Synthesis of hydrous zirconium oxide-impregnated chitosan beads and their application for removal of fluoride and lead," *Applied Surface Science*, vol. 372, pp. 13–19, 2016.

[296] C. B. Amphlett, L. A. McDonald, and M. J. Redman, "Synthetic inorganic ion-exchange materials—II: hydrous zirconium oxide and other oxides," *Journal of Inorganic and Nuclear Chemistry*, vol. 6, no. 3, pp. 236–245, 1958.

[297] N. I. Chubar, V. A. Kanibolotskyy, V. V. Strelko et al., "Adsorption of phosphate ions on novel inorganic ion exchangers," *Colloids and Surfaces A: Physicochemical and Engineering Aspects*, vol. 255, no. 1-3, pp. 55–63, 2005.

[298] S. M. Yakout and H. S. Hassan, "Adsorption characteristics of sol gel-derived zirconia for cesium ions from aqueous solutions," *Molecules*, vol. 19, no. 7, pp. 9160–9172, 2014.

[299] S. G. Botta, J. A. Navío, M:. C. Hidalgo, G. M. Restrepo, and M. I. Litter, "Photocatalytic properties of ZrO_2 and Fe/ZrO_2 semiconductors prepared by a sol-gel technique," *Journal of Photochemistry and Photobiology A: Chemistry*, vol. 129, no. 1–2, pp. 89–99, 1999.

[300] S. N. Basahel, T. T. Ali, M. Mokhtar, and K. Narasimharao, "Influence of crystal structure of nanosized ZrO_2 on photocatalytic degradation of methyl orange," *Nanoscale Research Letters*, vol. 10, no. 1, 2015.

[301] B. Pan, H. Qiu, B. Pan et al., "Highly efficient removal of heavy metals by polymer-supported nanosized hydrated

Fe(III) oxides: behavior and XPS study," *Water Research*, vol. 44, no. 3, pp. 815–824, 2010.

[302] T. A. Doncova, I. M. Astrelin, and J. N. Fedenko, "Regularities of cation sorption from water by an activated carbon-based nanocomposite," *Water and Ecology*, vol. 3, pp. 29–38, 2015.

[303] L. A. Zemskova, "Modified carbon fibers: sorbents, electrode materials, catalysts," *Bulletin of the Far Eastern Branch of the Russian Academy of Sciences*, vol. 144, no. 2, pp. 39–52, 2009.

[304] M. Shahadat, T. T. Teng, M. Rafatullah, and M. Arshad, "Titanium-based nanocomposite materials: a review of recent advances and perspectives," *Colloids and Surfaces B: Biointerfaces*, vol. 126, pp. 121–137, 2015.

[305] D. Papoulis, "Halloysite based nanocomposites and photocatalysis: a review," *Applied Clay Science*, vol. 168, pp. 164–174, 2019.

[306] T. R. Sahoo, *Polymer Nanocomposites for Environmental Applications*, in The Book: Properties and Applications of Polymer Nanocomposites, Springer, Germany, 2017.

[307] J. Zuo, X. Li, W. Jiang, X. Yang, and X. Wang, "Preparation of ZnO photocatalysts and study on photocatalytic degradation of antibiotic wastewater," in *Proceedings of the 4th International Conference on Mechatronics, Materials, Chemistry and Computer Engineering 2015*, pp. 2866–2869, Xi'an, China, 2015.

[308] F. S. Omar, H. Nay Ming, S. M. Hafiz, and L. H. Ngee, "Microwave synthesis of zinc oxide/reduced graphene oxide hybrid for adsorption-photocatalysis application," *International Journal of Photoenergy*, vol. 2014, Article ID 176835, 8 pages, 2014.

[309] S. Adhikari and D. Sarkar, "Preparation of mixed semiconductors for methyl orange degradation," *Journal of Nanomaterials*, vol. 2015, Article ID 269019, 8 pages, 2015.

[310] E. Llobet, "Gas sensors using carbon nanomaterials: a review," *Sensors and Actuators B: Chemical*, vol. 179, pp. 32–45, 2013.

[311] N. D. Hoa, N. van Quy, and D. Kim, "Nanowire structured SnO_x-SWNT composites: high performance sensor for NO_x detection," *Sensors and Actuators B: Chemical*, vol. 142, no. 1, pp. 253–259, 2009.

[312] S. Dhall and N. Jaggi, "Room temperature hydrogen gas sensing properties of Pt sputtered F-MWCNTs/SnO_2 network," *Sensors and Actuators B: Chemical*, vol. 210, pp. 742–747, 2015.

[313] G. Korotcenkov and B. K. Cho, "Metal oxide composites in conductometric gas sensors: achievements and challenges," *Sensors and Actuators B: Chemical*, vol. 244, pp. 182–210, 2017.

[314] H. Liang, F. Chen, R. Li, L. Wang, and Z. Deng, "Electrochemical study of activated carbon-semiconducting oxide composites as electrode materials of double-layer capacitors," *Electrochimica Acta*, vol. 49, no. 21, pp. 3463–3467, 2004.

[315] H. R. Rajabi, H. Arjmand, S. J. Hoseini, and H. Nasrabadi, "Surface modified magnetic nanoparticles as efficient and green sorbents: synthesis, characterization, and application for the removal of anionic dye," *Journal of Magnetism and Magnetic Materials*, vol. 394, pp. 7–13, 2015.

[316] S. C. N. Tang and I. M. C. Lo, "Magnetic nanoparticles: essential factors for sustainable environmental applications," *Water Research*, vol. 47, no. 8, pp. 2613–2632, 2013.

[317] N. A. Mikhailenko, O. V. Makarchuk, T. A. Dontsova, S. V. Horobets, and I. M. Astrilin, "Purification of aqeous media by magnetically operated saponite sorbents," *Eastern European Journal of Enterprise Technologies*, vol. 4, pp. 13–20, 2015.

[318] S. K. Giri, N. N. Das, and G. C. Pradhan, "Synthesis and characterization of magnetite nanoparticles using waste iron ore tailings for adsorptive removal of dyes from aqueous solution," *Colloids and Surfaces A: Physicochemical and Engineering Aspects*, vol. 389, no. 1-3, pp. 43–49, 2011.

[319] M. Hua, S. Zhang, B. Pan, W. Zhang, L. Lv, and Q. Zhang, "Heavy metal removal from water/wastewater by nanosized metal oxides: a review," *Journal of Hazardous Materials*, vol. 211-212, pp. 317–331, 2012.

[320] I. Larraza, M. López-Gónzalez, T. Corrales, and G. Marcelo, "Hybrid materials: magnetite-polyethylenimine-montmorillonite, as magnetic adsorbents for Cr(VI) water treatment," *Journal of Colloid and Interface Science*, vol. 385, no. 1, pp. 24–33, 2012.

[321] Z. Orolínová, A. Mockovčiaková, V. Zeleňák, and M. Myndyk, "Influence of heat treatment on phase transformation of clay-iron oxide composite," *Journal of Alloys and Compounds*, vol. 511, no. 1, pp. 63–69, 2012.

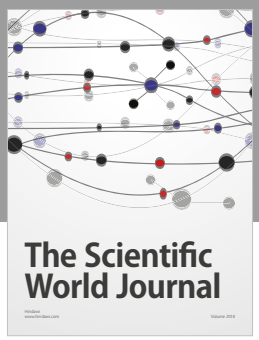

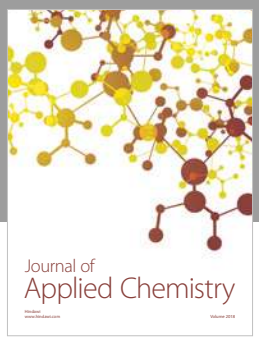

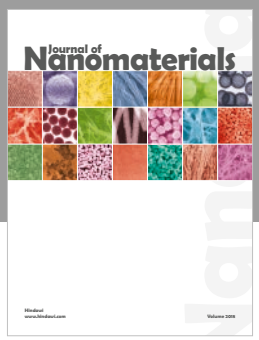

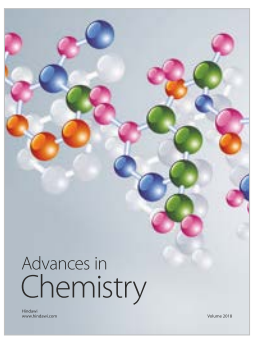

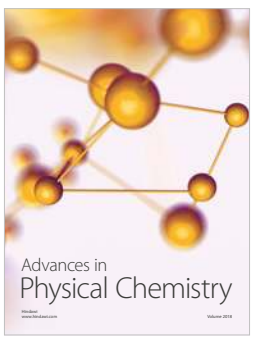

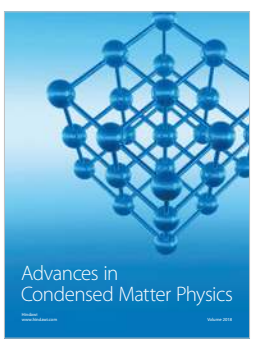

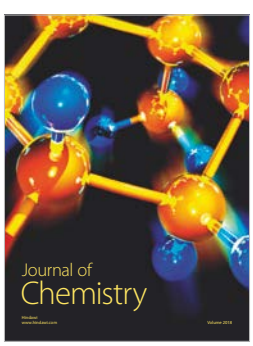

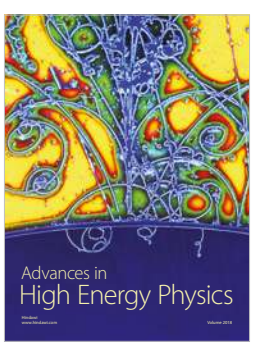

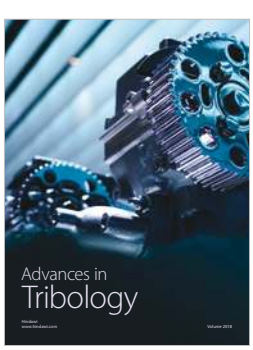

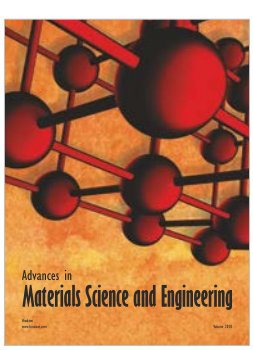

Hindawi

Submit your manuscripts at
www.hindawi.com